



RESEARCH ARTICLE

WILEY

The puzzling construction of the conidial outer layer of *Aspergillus fumigatus*

Isabel Valsecchi^{1,7,8} | Vincent Dupres² | Jean-Philippe Michel³ | Magalie Duchateau⁴ | Mariette Matondo⁴ | Georgios Chamilos⁵ | Cosmin Saveanu⁶  | J. Iñaki Guijarro^{7,8} | Vishukumar Aimaniananda¹ | Frank Lafont² | Jean-Paul Latgé¹ | Anne Beauvais¹ 

¹Aspergillus Unit, Institut Pasteur, Paris, France

²Centre for Infection and Immunity of Lille, Institut Pasteur de Lille-CNRS UMR8204-INSERM U1019-CHRU Lille-University, Lille, France

³UMR CNRS, Institut Galien Paris Sud, Châtenay-Malabry, France

⁴Plateforme Protéomique, Unité de Spectrométrie de Masse pour la Biologie, UMR 2000 CNRS, Institut Pasteur, Paris, France

⁵Department of Medicine, University of Crete and Institute of Molecular Biology and Biotechnology Foundation for Research and Technology, Crete, Greece

⁶Unité de Génétique des Interactions Macromoléculaires, Institut Pasteur, Paris, France

⁷Plateforme de RMN Biologique, Institut Pasteur (CNRS, UMR 3528), Paris, France

⁸Unité de bioinformatique structurale, Institut Pasteur (CNRS, UMR 3528), Paris, France

Correspondence

Anne Beauvais, Aspergillus Unit, Institut Pasteur, Paris 75015, France.
Email: anne.beauvais@pasteur.fr

Funding information

Agence Nationale de la Recherche, Grant/Award Numbers: ANR-10-EQPX-04-01 and FUNHYDRO ANR-16S-CE110020-01; Institut Pasteur Research Transversal Program PTR 529, Grant/Award Number: PTR 529

Abstract

If the mycelium of *Aspergillus fumigatus* is very short-lived in the laboratory, conidia can survive for years. This survival capacity and extreme resistance to environmental insults is a major biological characteristic of this fungal species. Moreover, conidia, which easily reach the host alveola, are the infective propagules. Earlier studies have shown the role of some molecules of the outer conidial layer in protecting the fungus against the host defense. The outer layer of the conidial cell wall, directly in contact with the host cells, consists of α -(1,3)-glucan, melanin, and proteinaceous rodlets. This study is focused on the global importance of this outer layer. Single and multiple mutants without one to three major components of the outer layer were constructed and studied. The results showed that the absence of the target molecules resulting from multiple gene deletions led to unexpected phenotypes without any logical additivity. Unexpected compensatory cell wall surface modifications were indeed observed, such as the synthesis of the mycelial virulence factor galactosaminogalactan, the increase in chitin and glycoprotein concentration or particular changes in permeability. However, sensitivity of the multiple mutants to killing by phagocytic host cells confirmed the major importance of melanin in protecting conidia.

KEYWORDS

Aspergillus, cell wall, chitin, galactosaminogalactan, glucan, hydrophobin, surface

1 | INTRODUCTION

The cell wall is a polysaccharide armor protecting the fungus against external aggressions including host defense mechanisms in case of pathogenic species. The cell wall of *Aspergillus fumigatus*, the most ubiquitous opportunistic fungal pathogen, has been extensively studied. It is mostly composed of a branched fibrillar β -(1,3)-glucan core linked to chitin and galactomannan, embedded in an amorphous matrix composed of α -(1,3)-glucan and galactomannan (Latgé &

Beauvais, 2014). Like all filamentous fungi, *A. fumigatus* adopts two different morphotypes: the spore and the mycelium. The asexual spore called conidium has a small size (3 μ m) and is the propagative morphotype. The ubiquity of the conidia in the atmosphere, their inhalation by every individuals and the fast growth rate of this species at 37°C are obvious biological causes for the induction of pulmonary pathologies in humans. The polysaccharide skeleton of the conidium is covered by a specific outer layer composed of melanin and proteinaceous rodlets (Latgé & Beauvais, 2014). Rodlet and melanin layers,

respectively, prevent the recognition of conidia by the host immune cells and confer resistance to killing (Aimanianda et al., 2009; Bayry et al., 2014; Fontaine et al., 2011). As soon as the conidium germinates, these melanin and rodlet layers are removed and the germinating conidia gets covered by α -(1,3)-glucans, which are responsible for the aggregation of germinating conidia during this process.

Early studies have shown the individual importance of these three cell wall components during infection and have pointed the different genes responsible for their biosynthesis. In contrast to spores covered with rodlets, hydrophilic conidia obtained by genetic or chemical removal of the RodA, the protein which forms the rodlet layer (Paris et al., 2003; Thau et al., 1994), are recognized by the innate immunity (Aimanianda et al., 2009).

Six-clustered gene products have been identified that mediate sequential catalysis of DHN-melanin biosynthesis (Bayry et al., 2014). The loss of melanin, resulting from the deletion of the first gene of the cluster, *PKSP*, ($\Delta pksP$ mutant) results in a major modification of the conidium cell wall. The $\Delta pksP$ mutant produces hydrophilic conidia due to the deposition of glycoproteins on their conidial surface (Bayry et al., 2014). $\Delta pksP$ is less virulent than the parental strain because immunostimulatory molecules, including the surface glycoproteins exposed in this mutant, activate a noncanonical autophagy pathway termed LC3-associated phagocytosis (LAP), which promotes phagolysosomal fusion and fungal killing. At the opposite, melanin blocks NADPH oxidase-dependent activation of LAP by excluding the p22phox NADPH oxidase subunit from the phagosomes (Akoumianaki et al., 2016).

α -(1,3)-Glucan also plays an important role in preserving the ultra-structure of the conidial surface (Beauvais et al., 2013). In *A. fumigatus*, they are synthesized by three α -(1,3)-glucan synthases, Ags1, 2, and 3 (Henry, Latgé, & Beauvais, 2012). Similarly to the $\Delta pksP$ mutant, the

$\Delta ags1$ - $\Delta ags2$ - $\Delta ags3$ (Δags) mutant, devoid of the cell wall α -(1,3)-glucan, produces hydrophilic conidia covered by glycoproteins. This mutant is less virulent than the parental strain due to exposed glycoprotein PAMPs, which results in a higher sensitivity to killing by phagocytes (Beauvais et al., 2013).

Because the individual removal of these three cell wall components, namely rodlets, melanin, and α -(1,3)-glucan, induces a modification of the *A. fumigatus* conidial surface which affected their virulence, we decided to generate mutants lacking different components of the outer layer to analyze the interplay and the impact of their removal on the conidium morphogenesis and interaction with the host immune cells.

2 | RESULTS

2.1 | Morphology of the conidia of the rodlet/melanin/ α -(1,3)-glucan mutants

Aspergillus fumigatus conidia are normally spherical, but oval shapes were frequently observed in the mutants deleted in *RODA* and/or *PKSP* analyzed in this study. Moreover, all mutant conidia with a *RODA* deletion aggregated as previously observed (Thau et al., 1994).

The color of the different mutant colonies is shown in Figure 1. After 3 weeks at 25°C on malt slants, the colonies are green in the Δags mutant like in the ku80 parental strain, white in the $\Delta pksP$ and ΔAP ($\Delta ags/\Delta pksP$) mutants, dark-green in the $\Delta rodA$ and ΔAR ($\Delta ags/\Delta rodA$) mutants and beige in the ΔPR ($\Delta pksP/\Delta rodA$) and ΔAPR ($\Delta ags/\Delta pksP/\Delta rodA$).

Deletion of *RODA* and/or *AGSs* (Δags , $\Delta rodA$, ΔAP , ΔAR , ΔAPR) led to a two-fold reduction in the number of conidia that were produced,

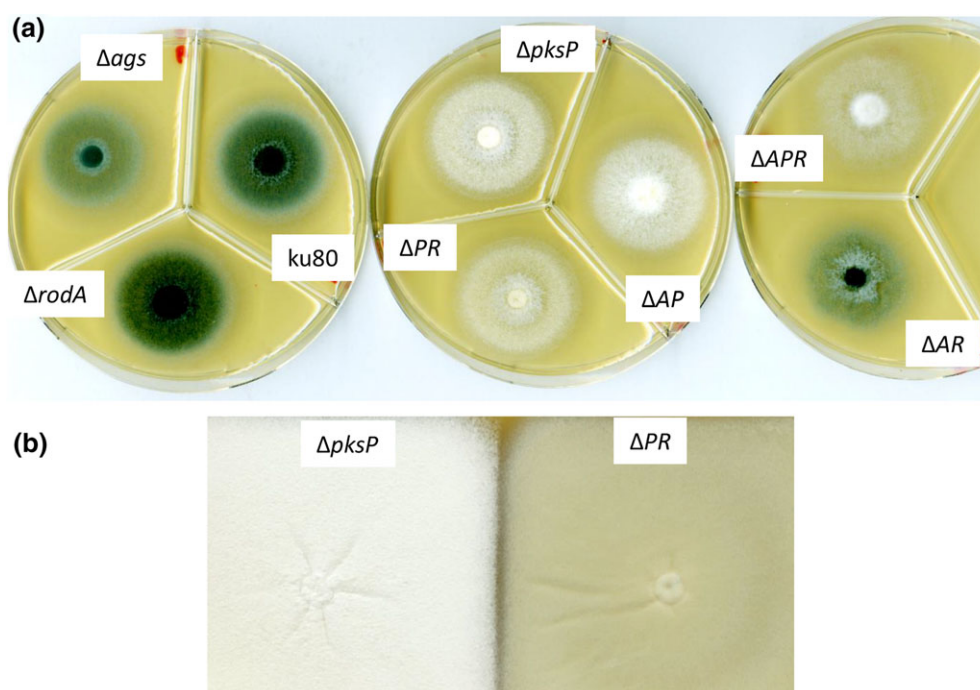


FIGURE 1 Phenotypical analysis of the mutants. (a) Sporulating cultures of parental and mutant strains on 2% (w/v) malt agar slants after 3 weeks at 25°C, showing the color of the conidia. Note the visible decrease in sporulation in Δags , ΔAP , ΔPR , ΔAR , and ΔAPR . The beige color of ΔPR and ΔAPR reinforced the impression of decrease in sporulation (B)

whereas the deletion of *PKSP* ($\Delta pksP$) did not affect conidiation (Figure 2). The double mutant ΔPR presented an intermediate phenotype with a 1.5x decrease in conidiation.

During the initial 2 hr of germination (wherein conidia start to swell isodiametrically), the melanin and rodlet layers are disrupted but are still present on the conidial surface until 3–4 hr (Dague, Alsteens, Latgé, & Dufrêne, 2008; Kyrnizi et al., 2018; Stappers et al., 2018). As the disruption of the melanin and rodlet layers is necessary for germination, it could be expected that mutant conidia lacking melanin and/or RodA would germinate faster. However, the $\Delta pksP$ or $\Delta rodA$ conidia germinated like the parental strain in Sabouraud medium (Figure 3). Contrastingly, all the conidia of mutants lacking α -(1,3)-glucan (Δags , ΔAP , ΔAR , and ΔAPR) germinated faster, indicating that only α -(1,3)-glucan but not melanin or RodA has an influence on the germination rate. These observations were confirmed also in GYE or MM media, which suggested that this phenomenon is not media specific (data not shown).

Many mutants with altered conidial phenotypes have been shown to be associated with a decreased survival over time in air or water (Henry et al., 2016; Millet, Latgé, & Mouyna, 2018; Valsecchi, Sarikaya-Bayram, et al., 2017). However, mutants altered in melanin, rodlets, and/or α -(1,3)-glucan did not present altered survival during extended storage in water or air (Figure S2).

2.2 | Cytochemical analysis of the conidial surface

The composition of the conidial surface was analyzed with different cytochemical tools: anti-RodA antibodies (Ab) to localize RodA, the MelLec-Fc receptor to detect melanin, FC-dectin 1 to localize β -(1,3)-glucan, B-4.1, or MOPC monoclonal Abs (mAbs) for α -(1,3)-glucan detection, EBA2 mAb to label galactofuranose-containing molecules (galactomannan or galactomannoproteins), anti-GAG mAb to localize galactosaminogalactan, Concanavalin A labeled with fluorescein isothiocyanate (ConA-FITC) to detect glycoproteins, and wheat germ agglutinin coupled to tetramethylrhodamine (WGA-TRITC) to

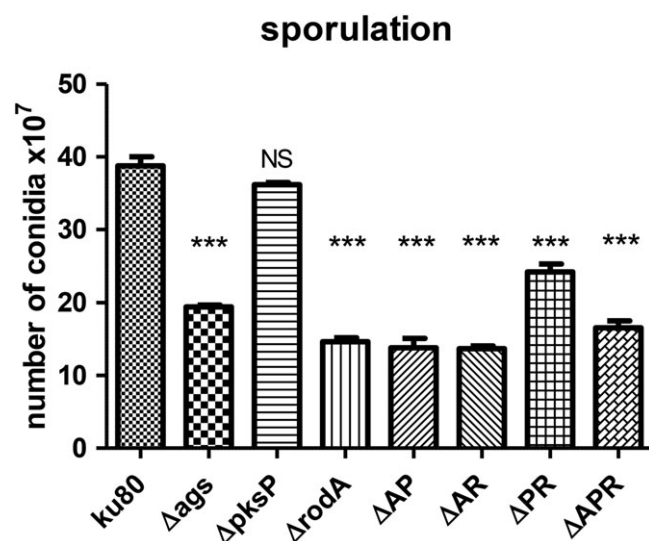


FIGURE 2 Sporulation of parental and mutant strains after 8 days at 25°C in 2% malt agar slants. *** $p < 0.001$

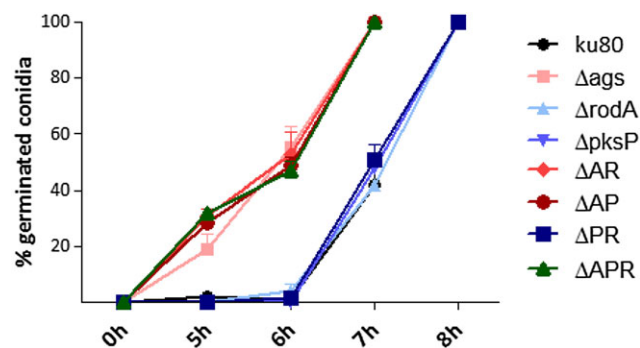


FIGURE 3 Germination of ku80 and mutant strains in Sabouraud medium, showing that the strains deleted in AGS genes germinated faster than ku80, $\Delta pksP$ or $\Delta rodA$

detect glucosamine (GlcNAc) polymers. Labeling results are summarized in Table 1.

2.2.1 | RodA detection

Despite the homogenous coverage of the surface by rodlets as observed by AFM, anti-RodA Abs labeled the ku80 conidial surface as patches, showing that the RodA epitopes recognized by the Abs were not uniformly present on the surface of the rodlets (Valsecchi, Dupres, et al., 2017). Conidia of *PKSP* or/and AGSs deletion mutants (Δags , $\Delta pksP$, and ΔAP) showed the same patchy immunolabeling as the ku80 parental strain (Figure 4). However, the RodA immunolabeling observed on ΔAP was weaker than on the Δags and $\Delta pksP$ mutants. Amorphous glycoproteins were previously observed on the surface layer of the Δags and $\Delta pksP$ mutants (Bayry et al., 2014; Beauvais et al., 2013). The lower accessibility of the antibody to the RodA epitopes on the ΔAP mutant suggested that a higher amount of proteins were present on the conidial surface of this mutant than on the single mutants Δags and $\Delta pksP$.

2.2.2 | Melanin detection

Δags mutant conidia showed a patchy melanin-labeling using an anti-Fc Ab binding to the MelLec-Fc receptor, as previously observed for the ku80 parental strain (Stappers et al., 2018). In contrast, labeling was uniform on the surface of the conidia of the *RODA* deleted mutants $\Delta rodA$ and ΔAR (Figure 5a). This result suggested that the melanin epitopes recognized by MelLec were mainly covered by rodlets. Of note, the patches that were positively labeled with the anti-RodA Abs and MelLec in the parental strain ku80 did not co-localize (Figure 5b).

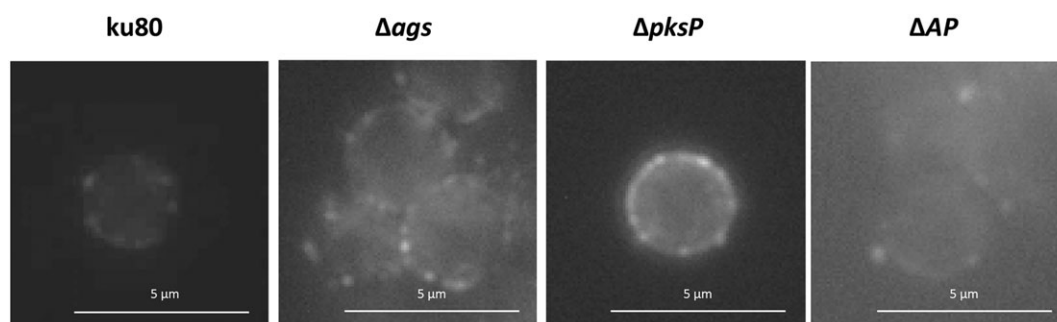
2.2.3 | Chitin and glycoproteins detection

As previously described (Bayry et al., 2014), $\Delta pksP$ was labeled by WGA-TRITC, whereas ku80 was not. Our results showed that Δags was not labeled by WGA-TRITC (data not shown), whereas $\Delta rodA$ was labeled (Figure 6). Similar to their parental strains, all the other mutants deleted in *PKSP* and/or *RODA* (ΔAP , ΔAR , ΔPR , and ΔAPR) were positive, indicating the presence of chitin on the conidial surface (data not shown).

TABLE 1 Analysis of the conidial surface composition of the mutants

Strain	RodA ^a	Melanin ^b	Glycoproteins ^c	Chitin ^d	GM ^e	β1,3 glucan ^f	α1,3 glucan ^g	GAG ^h
ku80	+, patches	+, patches	–	–	–	–	+	–
Δags	+, patches	+, patches	+++	–	–	–	–	–
ΔpksP	+, patches	–	+	+	–	–	–	–
ΔrodA	–	+, continue	–	+	–	+, 20%	–	–
ΔAP	+, patches	–	+	+	–	–	–	+
ΔAR	–	+, continue	++	+	–	+, 20%	–	–
ΔPR	–	–	++	+	–	+, 20%	–	–
ΔAPR	–	–	+	+	–	+, 20%	–	+

^aanti-RodA Abs and anti-mouse IgG-A488. ^bYWA1 detection by MelLec and anti-human Fc-IgG - Dylight 594. ^cConA-FITC. ^dWGA-TRITC. ^eanti-Galf Mab and anti-mouse IgG-A488. ^fFC-dectin1 and anti-human Fc-IgG-FITC. ^gB-4.1 and anti-mouse IgG-A488. ^hanti-GAG Mab and anti-mouse IgG-A488.

**FIGURE 4** RodA localization by immunolabeling with anti-rRodA Abs and anti-mouse IgG-Alexa 488 Abs

As shown before, conidia of the *Δags* and *ΔpksP* mutants were ConA-positive, whereas the parental strain ku80 was negative (Bayry et al., 2014; Beauvais et al., 2013). Similar to their parental strains, all the other mutants deleted in AGSs and/or PKSP genes (*ΔAP*, *ΔAR*, *ΔPR*, and *ΔAPR*) were positive indicating the presence of glycoproteins on the conidial surface of these mutants (data not shown). In contrast, *ΔrodA* was negative (data not shown).

2.2.4 | Galactofuranose (Galf) detection

Immunolabeling of the conidia using an anti-Galf mAb showed that the parental strain and all single mutants were negative. However, positive patches of fluorescence were observed on the conidia of the multiple mutants *ΔAP* and *ΔAPR* lacking α-(1,3)-glucan and melanin, indicating the presence of galactomannan or galactomannoproteins on the surface of these conidia (Figure 7).

2.2.5 | β-(1,3)-Glucan detection

Dectin 1-Fc interacted with only 20% of the surface of all the mutants lacking the *RODA* gene (*ΔrodA*, *ΔAR*, *ΔPR*, and *ΔAPR*) (Figure 8). The parental strain ku80 and the *Δags*, *ΔpksP*, and *ΔAP* mutants were not labeled with the β-(1,3)-glucan-receptor dectin 1.

2.2.6 | α-(1,3)-Glucan detection

The two anti α-(1,3)-glucan-mAbs B-4.1 and MOPC, with different recognition specificity (Beauvais et al., 2013), were used to label α-(1,3)-glucan (Figure 9). Only B-4.1 showed a weak but positive

immunolabeling in patches on ku80 dormant conidia, whereas MOPC immunolabeling was negative. This result suggested that the epitope recognized by B-4.1 was accessible on the conidia conversely to the MOPC epitope which has been shown to be accessible on the mycelium surface. Conidia of all single and multiple mutants were negative with the B-4.1 and MOPC mAbs (data not shown).

2.2.7 | Galactosaminogalactan (GAG) detection

It has been previously demonstrated that galactosaminogalactan (GAG) is absent in conidia but present in the mycelium cell wall (Fontaine et al., 2011). However, immunolabeling of the conidia using an anti-GAG mAb showed that conidia without α-(1,3)-glucan and melanin (*ΔAP* and *ΔAPR*) were positively labelled with the anti-GAG mAb (Figure 10a). The immunolabeling data were confirmed biochemically after cell wall fractionation and HCl hydrolysis of the conidial cell wall fractions, showing that 5% galactosamine, indicative of the GAG molecule, was indeed present only in the *ΔAP* and *ΔAPR* alkali-soluble fraction (Figure 10b).

In conclusion, single, double, or multiple deletion of genes coding for the synthesis of α-(1,3)-glucan, rodlets, and melanin resulted in the modification of the surface of the conidium and the exposition of glycoproteins, β-(1,3)-glucan, chitin, galactomannan, and GAG, normally absent from the surface of the parental strain. Exposure of these different molecules varies with the genes deleted. Moreover, multiple gene deletion does not lead to an additivity of the phenotypes resulting from the successive deletions as shown in Table 1. In addition, the observed compensatory cell wall composition can be totally

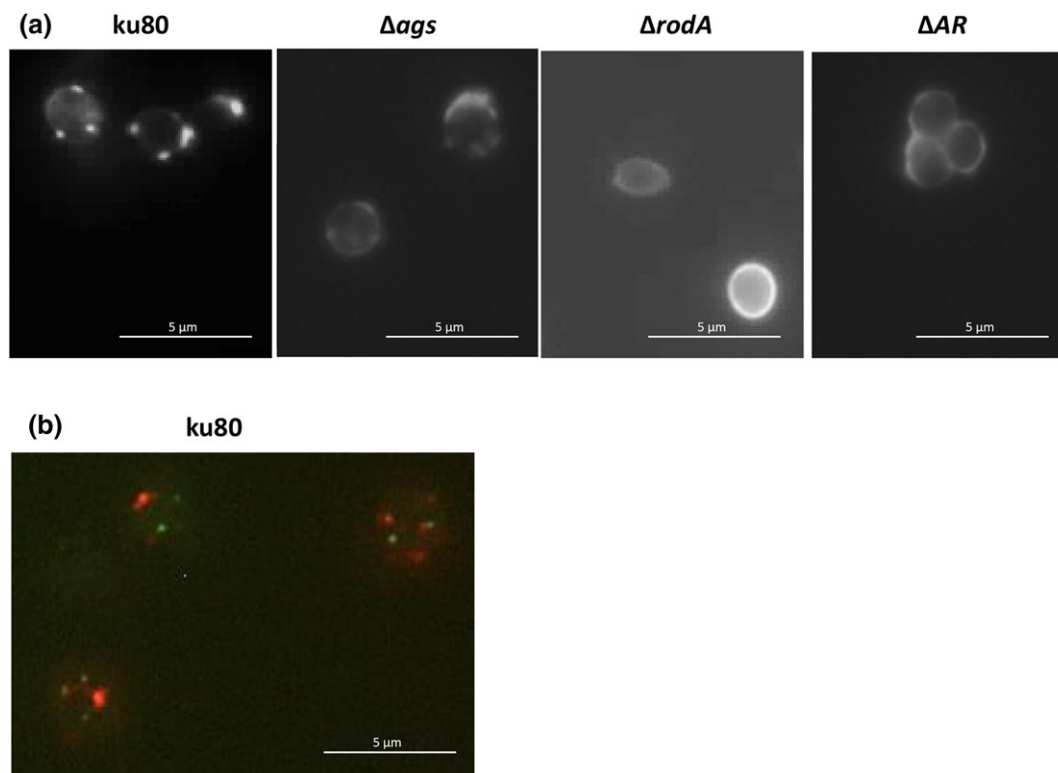


FIGURE 5 Melanin localization. (a) Detection in ku80 and the melanin containing mutant conidia with the human MelLec melanin-receptor conjugated to Fc-IgG and anti-human Fc-IgG-dylight 594 Abs. (b) Co-localisation of melanin (red) and RodA (green) on the conidia of the ku80 strain, labeled as above and as described in Figure 4 respectively

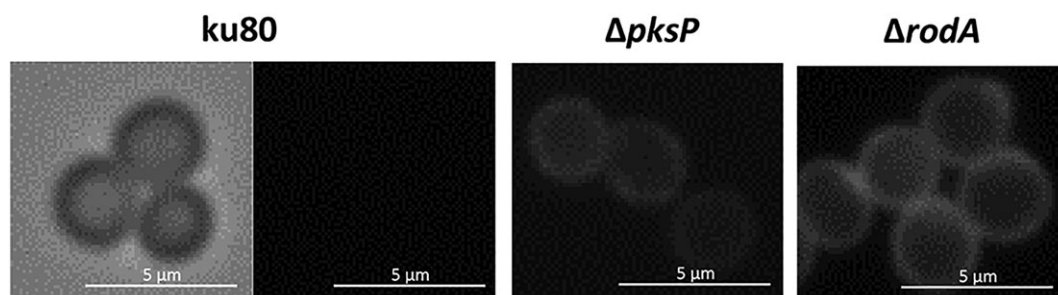


FIGURE 6 Chitin detection with WGA-TRITC on the conidial surface of $\Delta pksP$ and $\Delta rodA$ mutants

unexpected as in the case of the ΔAP and ΔAPR mutants in which the lack of α -(1,3)-glucan and melanin is the secretion of GAG, which is characteristically not synthesized in *A. fumigatus* wild type conidia.

2.3 | Surface proteins extracted with formic acid

Around 300 proteins were extracted from conidia of the parental strain ku80 after 10 min incubation in 60% formic acid (Figure 11a). These proteins were also recovered in the formic acid extracts from all mutants. In addition to these 300 common proteins, which were extracted from all strains, 700 to 2,000 supplementary and unique proteins were extracted from the mutant conidia with formic acid (Figure 11a). The highest number of protein were found in ΔAP and ΔAR mutants with around 2,000 proteins being identified in these mutants. Figure 11b gives an estimate of the concentration of the

proteins extracted from conidia, based on the number of peptides and intensity calculated by the Mas quant software (Bubis, Levitsky, Ivanov, Tarasova, & Gorshkov, 2017). It indicated that the amount of total proteins extracted was the highest in the multiple mutants. No specific protein signature could be determined for each mutant (<http://www.proteomexchange.org/px> submission #309081; Table S1). However, Table S1 showed that RodA gave the most intense signal in ku80 strain.

Hydrophobins RodA, RodB, and RodC, and some secreted antigens are known to be present in the conidial cell wall (Valsecchi, Dupres, et al., 2017). Previous studies have shown that after strong acid extraction (48% hydrofluoric acid for 72 hr at 0°C), similar levels of RodA were found in ku80, Δags , and $\Delta pksP$ (Bayry et al., 2014; Beauvais et al., 2013). In our conditions of mild acid extraction (60% formic acid, 10 min, 0°C), the relative level of RodA was lower in Δags , $\Delta pksP$, and ΔAP than in ku80 (Figure 12a). With the exception of the

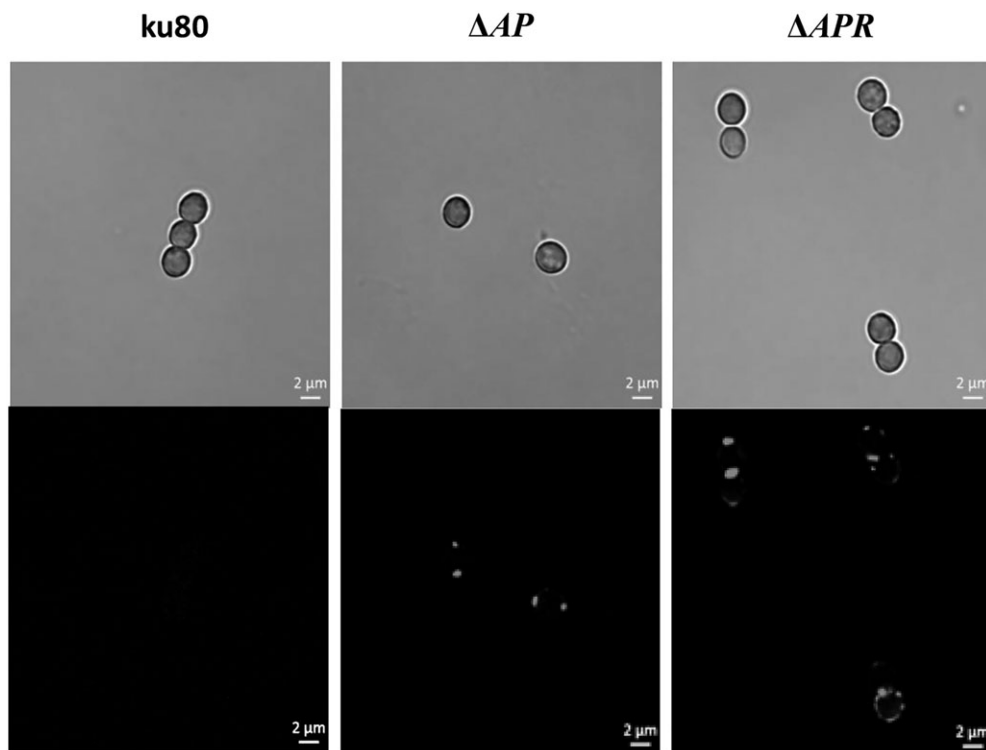


FIGURE 7 Punctuated labelling on ΔAP and ΔAPR conidia with anti-galactofuranose mAb and anti-rat IgG-FITC Abs

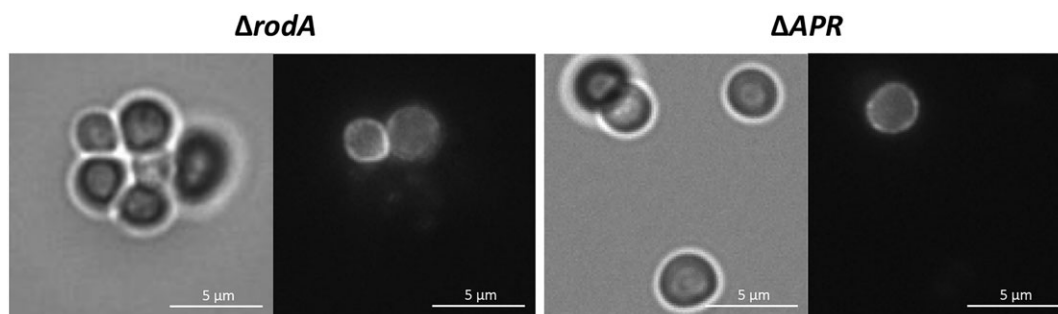


FIGURE 8 β -(1,3)-Glucan localization on $\Delta rodA$ and ΔAPR conidia by the human β -(1,3)-glucan receptor dectin1 conjugated to Fc-IgG and anti-human Fc-IgG-dylight 594 Abs. Note that dectin-1-Fc did not interact with all conidia

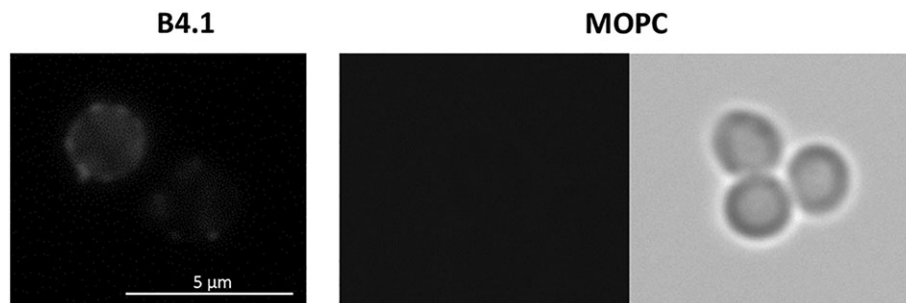


FIGURE 9 α -(1,3)-Glucan localization by B-4.1 or MOPC and anti-mouse IgG-Alexa 488 Abs on ku80 conidia, showing that only B-4.1 interacted with the conidia

ΔPR strain, the amount of RodB was similar in all strains including ku80 (Figure 12a). The same amount of RodC was recovered in ku80 and $\Delta rodA$ extracts. This hydrophobin was less extracted from other mutants and the lowest levels were detected in ΔPR and ΔAPR mutants (Figure 12a). It is interesting to note that the deletion of RodA

in $\Delta rodA$, ΔAR , ΔPR , and ΔAPR did not induce a higher expression of RodB or RodC (Figure 12a).

Antigens such as Alp1 (AFUA_4G11800), Alp2 (AFUA_5G09210), AspF1 (AFUA_5G02330), AspF13 (AFUA_4G11800), and DPPV (AFUA_2G09030) are known to accumulate in the conidial cell wall

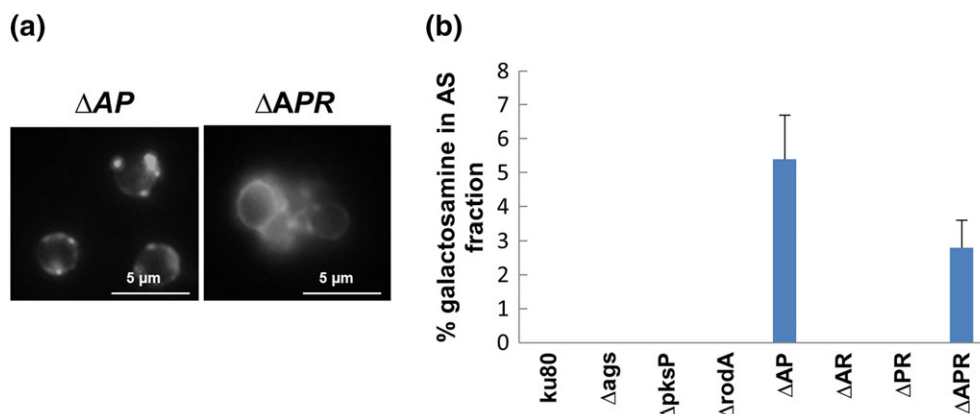


FIGURE 10 Detection of GAG on ΔAP and ΔAPR conidia. (a) Detection with anti-GAG mAbs and anti-mouse IgG-Alexa 488 Abs. (b) Biochemical GAG detection by HCl hydrolysis of the conidial cell wall alkali-soluble (AS) fractions of parental and mutant strains

before being secreted during swelling of conidia and hyphal growth (Lamarre et al., 2008; Singh et al., 2010). The antigens mentioned above and Con10, a conidial cell wall of unknown function (Suh et al., 2012), were recovered in higher amounts in the formic acid extracts of the mutants than of ku80, suggesting a higher permeability of the mutant conidial cell wall compared with ku80 (Figure 12b).

2.4 | Hydrophobicity of the mutant conidia

The surface of the conidia was inspected by AFM (Figure 13). Rodlets were easily observed on the ku80 parental strain. In contrast, and as published previously (Thau et al., 1994), the surface of the conidia of the rodlet-less mutant $\Delta rodA$ was totally amorphous. Like the $\Delta rodA$ mutant, the conidia of the ΔAR , ΔPR , and ΔAPR mutants displayed an amorphous surface. The conidia of the Δags , $\Delta pksP$, and ΔAP showed an intermediate phenotype with rodlets and amorphous material covering their surface. The hydrophobicity of the surface was quantified with a hydrophobic tip (Figure 14a). For the parental strain ku80, the mean rupture force (MRF) by the hydrophobic tip presented an average of 1,600 pN. At the opposite, $\Delta rodA$ presented a ~10-fold lower MRF (170 pN). ΔAR and ΔPR also presented weak MRFs (~260 and ~290 pN respectively). The MRF values of Δags and $\Delta pksP$ were intermediate (470 and 420 pN respectively) in agreement with the presence of an amorphous material partially covering the rodlet layer. Surprisingly, the MRF values of ΔAP and ΔAPR were ~920 and ~730 pN respectively, which are higher than the values seen with the other single or multiple *RODA* deleted mutants ($\Delta rodA$, ΔAR , and ΔPR) and their respective parental Δags and $\Delta pksP$. Because GAG was observed on the surface of these two mutants (Figure 10) and is known to be very sticky (Beaussart, El-Kirat-Chatel, Fontaine, Latgé, & Dufrêne, 2015; Gravelat et al., 2013), this could explain the high rupture force obtained in AFM with ΔAP and ΔAPR mutants. To verify this hypothesis, AFM was performed on GAG using the same hydrophobic tip used for conidia, and indeed, the rupture force on GAG was 3 nN (data not shown).

The hydrophobicity of the conidia was also estimated by their ability to sink in water (Figure 14b). All mutants deleted in *RODA* ($\Delta rodA$, ΔAR , ΔPR , and ΔAPR) were completely hydrophilic, whereas

the parental ku80 strain was highly hydrophobic and floated on the water surface. The Δags , $\Delta pksP$, and ΔAP mutants presented an intermediate phenotype. It is interesting to observe that hydrophilic mutant lost the ability to be dispersed in air (data not shown).

The modification of the surface composition and structure of mutant conidia could also affect the adherence of conidia to hydrophobic surfaces. To test this hypothesis, conidia were washed, resuspended in water and adherence was directly tested on a polystyrene plate during 1 hr before extensive washing. Conidia without melanin (deleted in *PKSP*), mostly in combination with *RODA* and/or *AGSs*, presented increased adherence (Figure 15), which could be due to interactions of the proteins present on the surface of $\Delta pksP$ conidia and polystyrene.

2.5 | Susceptibility to anti *A. fumigatus* chemicals and phagocyte effectors

2.5.1 | Azoles

The minimal inhibitory concentrations (MICs) of all mutant and parental ku80 strains were similar for voriconazole (0.4 $\mu g/ml$). For posaconazole, the MIC was 48–96 ng/ml for all strains except for ΔAPR , which was slightly more resistant to the drug with a MIC of 96–120 ng/ml ($p = 0.09$).

2.5.2 | Congo red and calcofluor white

The Δags mutant was more sensitive to congo red (CR) and calcofluor white (CFW) with MIC values of 20 and 30 $\mu g/ml$, respectively, compared with the parental strain ku80 (MIC values: CR 100 $\mu g/ml$, CFW 80 $\mu g/ml$; Table 2). The mutants ΔAP and ΔAR behaved like Δags strain. At the opposite, the absence of rodlets or melanin in $\Delta rodA$ or $\Delta pksP$, respectively, rendered the conidia of these mutants more resistant to CR and CFW than the parental strain (MIC values of 300 and 100 $\mu g/ml$, respectively) as shown in Table 2. Their derived mutants ΔPR and ΔAPR , behaved like the corresponding parental strains, $\Delta rodA$ and $\Delta pksP$, in spite of the deletion of *AGS* genes in ΔAPR .

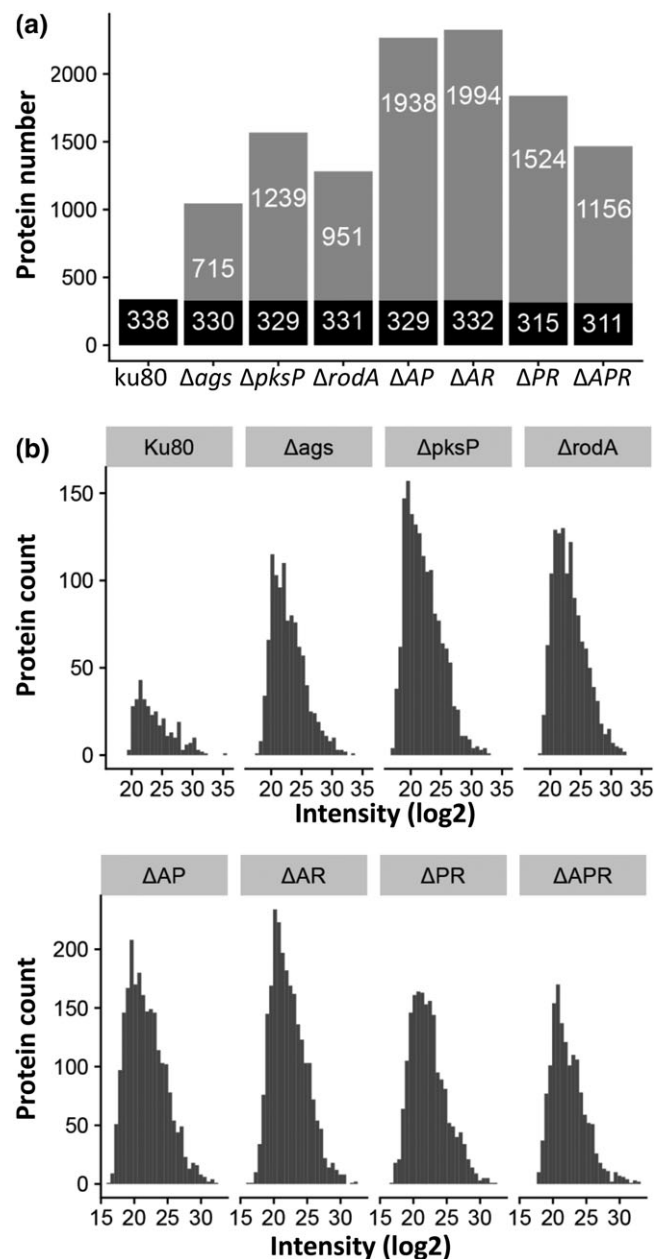


FIGURE 11 Number of proteins identified in the parental strain and the seven mutants constructed. Conidia were incubated in 60% formic acid for 10 min on ice, and the protein extracted in the supernatant were identified by LC-MS/MS. (a) The number of proteins reliably identified in at least two replicate experiments was consistently higher in mutant strain extracts than in the parental strain (ku80). Each of the bars represents the number of identified proteins, with black zones highlighting the number of proteins present in the ku80 extract and also identified in each mutant strain extract. (b) Distribution of signal intensity for the proteins identified in the parental and mutant strains

2.5.3 | Caspofungin

All mutants deleted in AGSs (Δags , ΔAP , ΔAR , and ΔAPR) were resistant to caspofungin, showing a CME > 30 $\mu\text{g}/\text{ml}$ compared with the CME 0.24–0.48 $\mu\text{g}/\text{ml}$ of ku80, $\Delta rodA$ and ΔPR , and 15 $\mu\text{g}/\text{ml}$ of $\Delta pksP$ (Table 2). It is interesting to observe that the $\Delta pksP$ conidia showed a different sensitivity curve to ku80 or the mutant ΔPR (Figure S3).

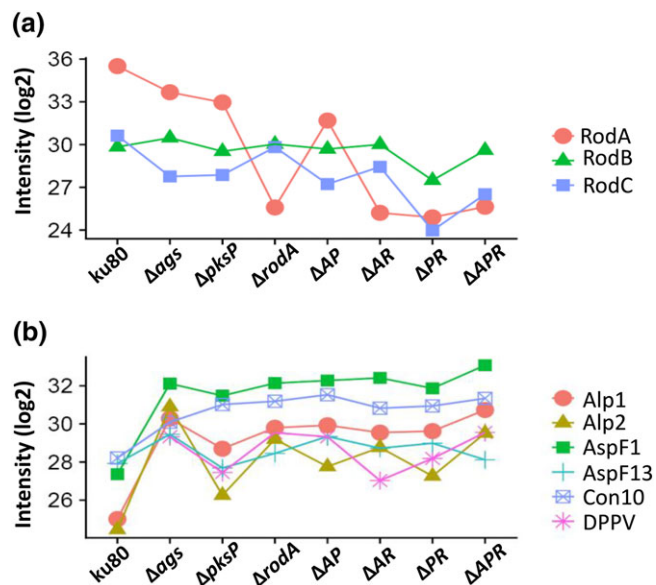


FIGURE 12 Intensity profiles for specific conidial proteins (extracted as described in Figure 11) based on mass-spectrometry. (a) Normalized intensity values of the hydrophobins RodA, RodB, and RodC in the parental and mutant cell extracts obtained under identical conditions from different strains. Intensity values for RodA in the strains where the corresponding gene was deleted (due to contaminations on columns used during LC-MS/MS by RodA from other RodA-containing strain extracts), corresponded to background values (0.1% of the signal when RodA is present in the strain). (b) A selection of proteins that were identified in the ku80 extract and varied in intensity in the mutant strain extracts: Alp1 and Alp2 are alkaline proteases, AspF1 and AspF13 are known *Aspergillus* allergens, Con10 is a conidiation specific protein and DPPV is the dipeptidyl-peptidase V

2.5.4 | Monocytes

Ex vivo experiments with human monocytes allowed us to investigate the killing of conidia by phagocytes and the associated LC3 recruitment in *A. fumigatus* phagosomes. As previously demonstrated, $\Delta rodA$, or the isogenic parental strain ku80 resulted in low and comparable rates of LC3 phagosome recruitment, without an apparent activation of the specialized form of autophagy termed LAP over time (Figures 16a, Figure S4; Akoumianaki et al., 2016). LC3 recruitment to the phagosome correlated with NADPH oxidase assembly assessed by p47phox staining and ROS production (Figure 17). Finally, other than melanin, there was no evidence of another molecule with inhibitory action on LAPosome formation. Importantly, the results on activation of LAP correlated with the susceptibility of mutants to killing by primary human monocytes. Specifically, the efficiency of killing of conidia of *PKSP* deleted strains by monocytes was significantly higher when compared with killing of isogenic parental ku80 strain, Δags , and $\Delta rodA$ (Figure 16b). Collectively, the multiplicity of the deletion of the rodlet, melanin, and α -(1,3)-glucan did not aggravate the sensitivity of the conidia to the phagocyte killing (Figure 16b) and indicated that melanin was the major cell wall component protecting the conidia against host defence reaction.

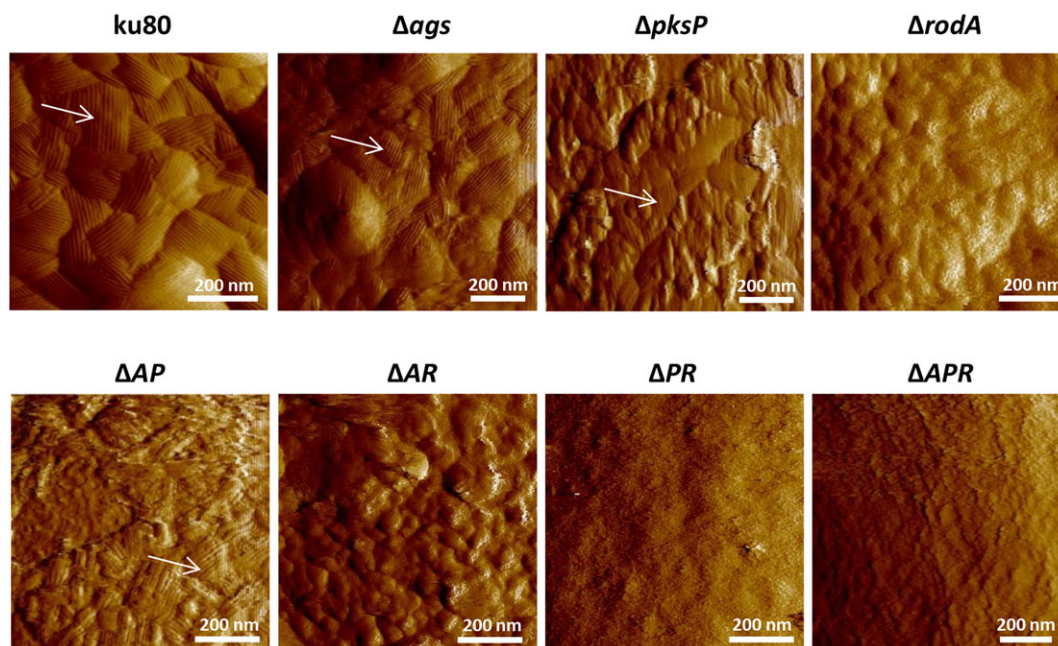


FIGURE 13 AFM images showing the presence of rodlets (arrows) all over the conidial surface of ku80 parental strain and partly on the surface of Δ ags, Δ pksP, and Δ AP, whereas the conidial surfaces of strains deleted in RODA are amorphous

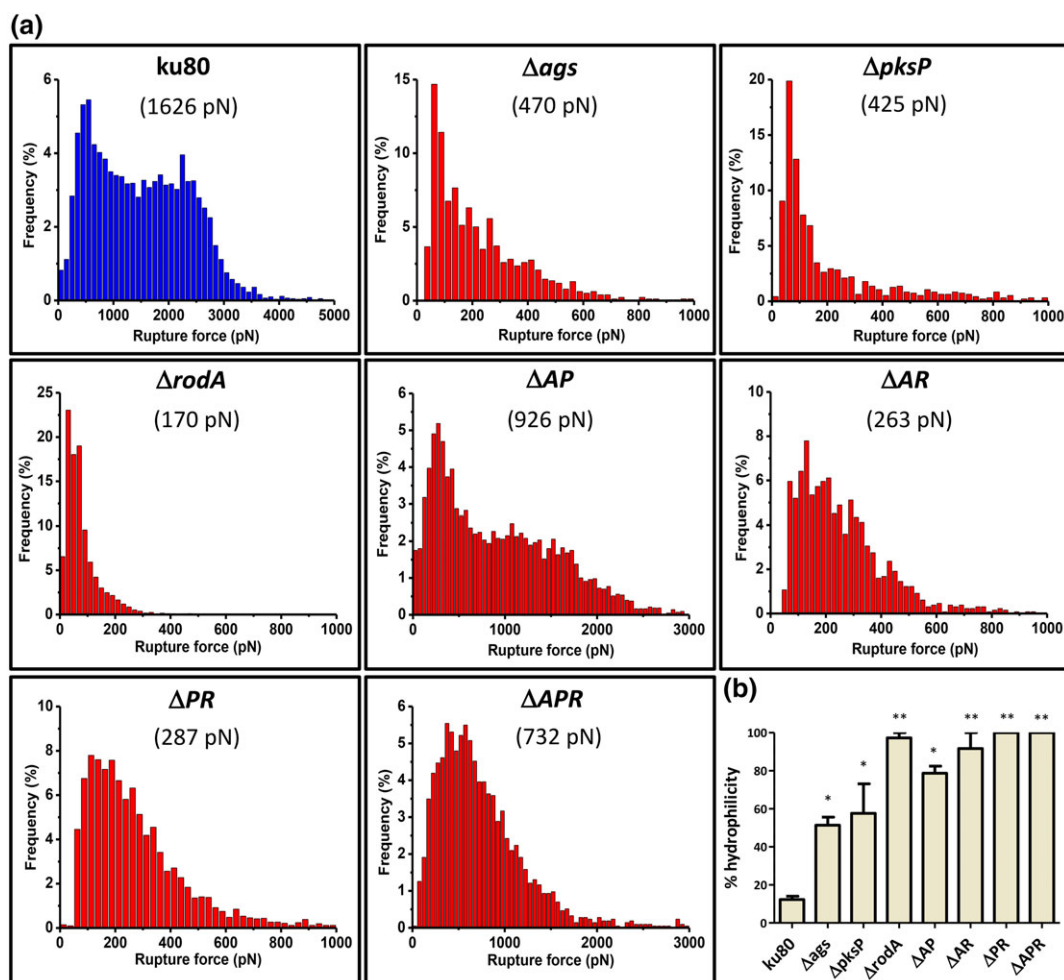


FIGURE 14 Hydrophobicity of parental and mutant conidia. (a) Mean rupture forces (pN) measured by a hydrophobic tip under AFM. Note that the scale of the X-axis is different for different mutants. (b) Percent of hydrophilicity of the conidia in water. * $p < 0.02$; ** $p < 0.002$

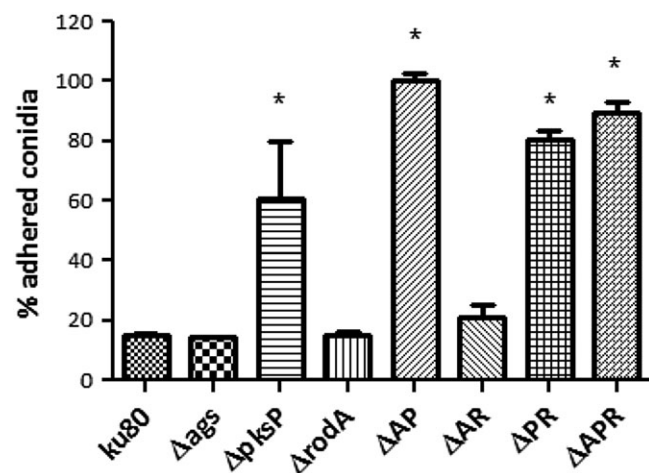


FIGURE 15 Adherence of mutant and parental conidia to polystyrene after 1 hr, showing that all mutants deleted in *PKSP* were more adherent. * $p < 0.02$

2.6 | Permeability of the cell wall of the mutants to drugs

The modification of the cell wall permeability in the different mutants using pyocyanin, CAS-DDAO, and liposomes as markers of permeability is summarized in Table 3.

2.6.1 | Pyocyanin

The resting conidia of melanin knockout mutants ($\Delta pksP$, ΔAP , ΔPR , and ΔAPR) were permeable to pyocyanin with dots of the auto-fluorescent pyocyanin intracellularly in the conidia of these mutants (Figure 18). In contrast, the resting conidia of the Δags , $\Delta rodA$, and ΔAR mutants and the parental strain ku80 were not permeable to pyocyanin (Figure 18 and data not shown). After swelling, however, these mutant and parental strains became permeable to pyocyanin (Figure 18 and data not shown). The intracellular labeling of the $\Delta pksP$, ΔAP , ΔPR , and ΔAPR conidia showed increased intensity after 2 hr of germination (Figure 18).

2.6.2 | DDAO-caspofungin

We analyzed the permeability of all strains to caspofungin conjugated to DDAO (CAS-DDAO). The experiment was done on germinated

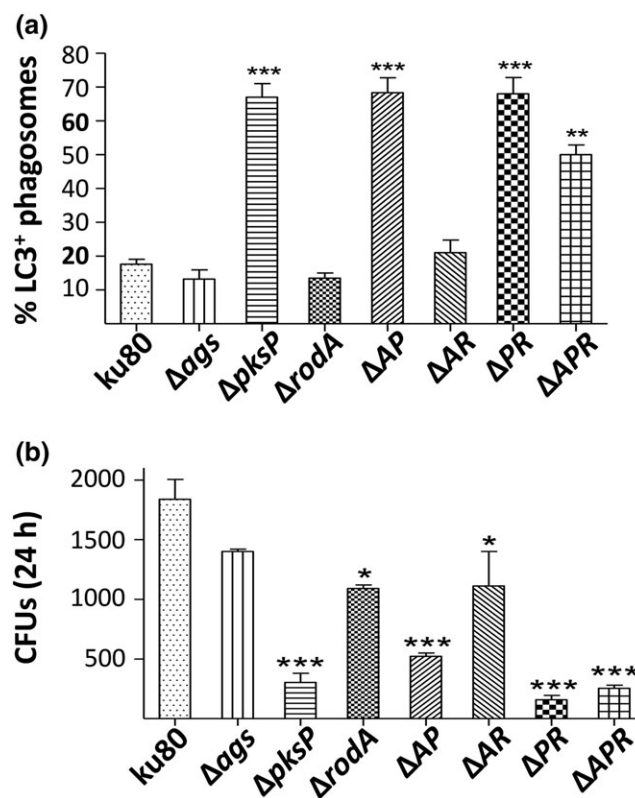


FIGURE 16 Primary human monocytes were infected with FITC-labeled live dormant conidia of the indicated *Aspergillus fumigatus* strain for 1 hr at 37°C at an MOI of 1:10 (fungus:cell). Cells were stained for LC3 (red) and TOPRO-3 (blue, nuclear staining) and analyzed by confocal microscopy (Figure S4). (a) Quantification of LC3+ phagosomes are presented as mean \pm SEM of three independent experiments. (b) After removing non-adherent and nonphagocytosed conidia, and addition of new medium, killed conidia after 24 hr culture of the monocytes were assessed by CFU counts. Data are presented as mean \pm SEM of one out of four independent experiments performed in triplicate ($n = 3$). * $p < 0.02$; *** $p < 0.0001$

conidia because it was not possible to see CAS-DDAO in dormant conidia as previously shown (Pratt et al., 2013). At 7 μ M of CAS-DDAO, 3–17% germinated conidia of the α -(1,3)-glucan deficient strains were fluorescent compared with 30% to 65% for ku80, $\Delta rodA$, $\Delta pksP$, and ΔPR (Figure 19). In all positive germinated conidia, the labeling with 7 μ M of CAS-DDAO was intracellular. Even though caspofungin has been shown to act on the extracellular domain of the β -(1,3)-glucan synthase localized in the plasma membrane (Johnson & Edlind, 2012), previous studies showed that

TABLE 2 CMI/CME values of mutant and the parental strains incubated in presence of voriconazole, posaconazole, congo red, and calcofluor white (CMIs), caspofungin (CME) for 48 h at 37°C in MM medium

	ku80	$\Delta ags123$	$\Delta pksP$	$\Delta rodA$	ΔAP	ΔAR	ΔPR	ΔAPR
Voriconazole (μ g/ml)	0.4	0.4	0.4	0.4	0.4	0.4	0.4	0.4
Posaconazole (ng/ml)	48–96	48–96	48–96	48–96	48–96	48–96	48–96	96–120
Calcofluor white (μ g/ml)*	80	30	100	100	20	30	90	100
congo red (μ g/ml)*	100	20	300	300	20	40	250	300
Caspofungin (μ g/ml)	0.24–0.48	> 30	15	0.24–0.48	> 30	> 30	0.24–0.48	> 30

*MIC differences of CR and CFW for the mutants were statistically significant to the MICs of ku80.

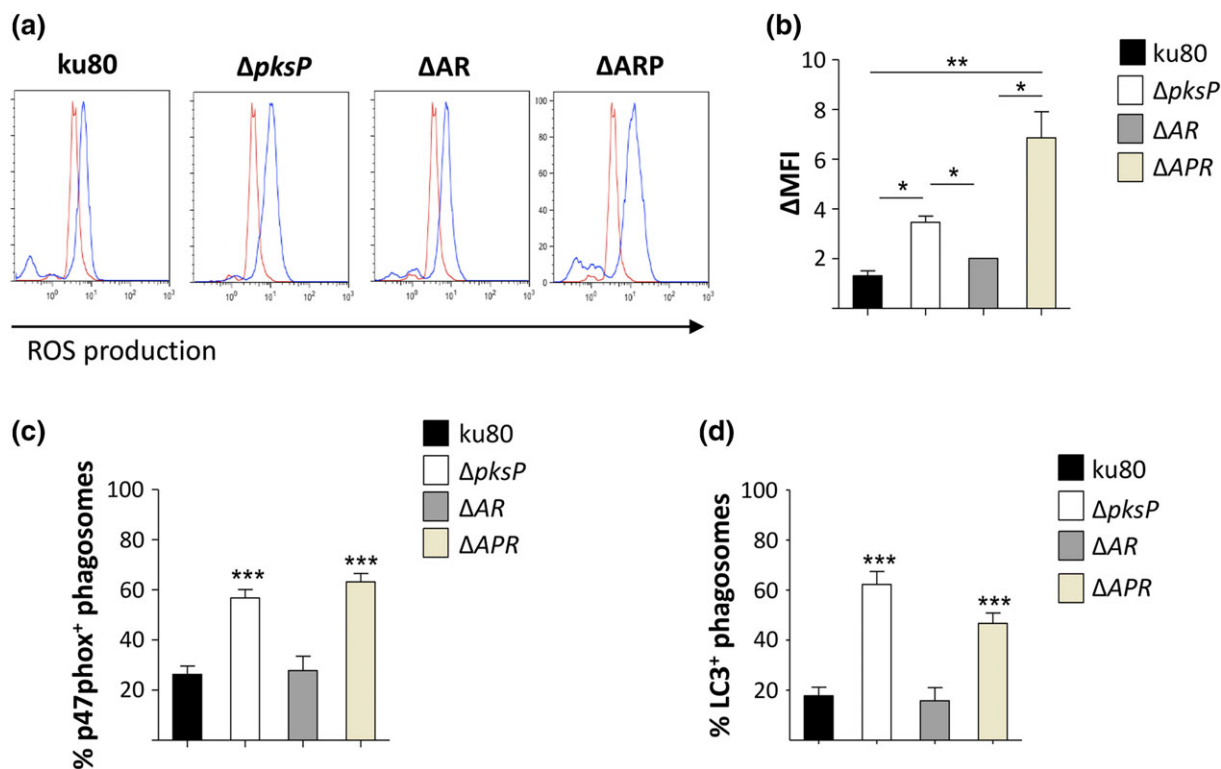


FIGURE 17 NADPH oxidase-dependent activation of LC3-associated phagocytosis in primary human monocytes infected for 30 min with pFA fixed-conidia of the indicated *Aspergillus fumigatus* strain. (a,b) Intracellular ROS production in the monocytes determined by measurement of relative fluorescent intensity of DCFH-DA. Representative FL1 histograms are shown in (a). Differences in ROS production between experimental groups are presented as mean \pm SEM from three independent experiments (b). (c,d) Data on quantification of p47phox⁺ (c), and LC3⁺ (d) in the monocytes, presented as mean \pm SEM of one out of three independent experiments. *p < 0.01, **p < 0.001, ***p < 0.0001

TABLE 3 Selective permeability of resting and germinating conidia to pyocyanin, DDAO-labeled caspofungin and FITC-liposomes 50 nm

Strain	Pyocyanin		DDAO-Caspofungin		POPC/DSPE-NBD liposomes	
	resting	germinating	resting	germinating	resting	germinating
ku80	–	+	–	+	–	–
Δags	–	+	–	–	–	+
$\Delta pksP$	+	+	–	+	–	–
$\Delta rodA$	–	+	–	+	–	–
ΔAP	+	+	–	–	–	+
ΔAR	–	+	–	–	–	+
ΔPR	+	+	–	+	–	–
ΔAPR	+	+	–	–	–	+

exposure to growth-inhibitory concentrations of caspofungin causes a mislocalization of the β -(1,3)-glucan synthase to vacuoles (Moreno-Velázquez, Seidel, Juvvadi, Steinbach, & Read, 2017). Inhibitory concentrations of caspofungin resulted in repeated lysis of apex compartments as seen upon incubation of the ku80, $\Delta rodA$, $\Delta pksP$, and ΔPR mutants with 7 μ M of CAS-DDAO (Figure 19). In contrast, lysis was never observed in germ tubes of Δags , ΔAP , ΔAR , and ΔAPR .

2.6.3 | POPC/DSPE-NBD liposomes

The permeability of the mutants was assessed with 50 nm POPC/DSPE-NBD liposomes. Dormant conidia were impermeable to POPC/DSPE-NBD liposomes (data not shown). The permeability of

the swollen conidia to liposomes was totally opposite to the one seen with CAS-DDAO: Δags , ΔAP , ΔAR , and ΔAPR were permeable to POPC/DSPE-NBD liposomes whereas ku80, $\Delta rodA$, $\Delta pksP$, and ΔPR were not (Figure 20).

The conclusion of this permeability analysis is shown in Table 3. The permeability of the conidial cell wall was affected in the different mutants. No definite, however, could be established because our results showed that the modification of permeability depends on both the cell wall components missing and the drug used to test the permeability of the cell wall. Liposomes can penetrate the germinated conidia of the α -(1,3)-glucan-less mutants, whereas the same mutants became impermeable to caspofungin. In contrast, the resting conidia mutants without melanin were permeable to pyocyanin.

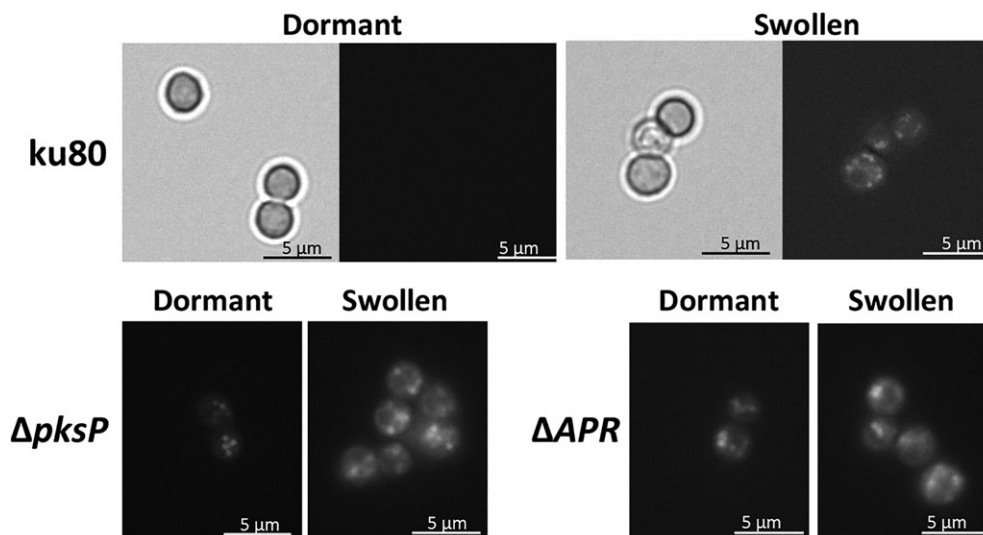


FIGURE 18 Permeability to pyocyanin of *ku80*, $\Delta pksP$, and ΔAPR in dormant or swollen conidia, showing that *PKSP* deleted conidia are more permeable

2.7 | Interactions between α -(1,3)-glucan, melanin, and rodlets

Mutants were used to investigate if rodlets, melanin, and α -(1,3)-glucan were linked together on the cell wall. Each deletion mutant was complemented with the missing component. *RODA* knockout mutants were complemented with soluble monomeric recombinant rRodA. Because α -(1,3)-glucan and melanin polymers are water-insoluble, AGS deleted mutants were complemented with α -(1,3)-glucan-oligomers containing 7, 9, or 11 glucose units and melanin knockout mutants with the heptaketide naphthopyrone molecule YWA1, which is the first intermediate of the melanin synthesis pathway and the MelLec binding molecule (Stappers et al., 2018). α -(1,3)-Glucan-oligomers did not bind to AGS deleted mutants (Δags , ΔAP , ΔAR , and ΔAPR , data not shown). In contrast, rRodA and YWA1 bound to *RODA* and *PKSP* deleted mutants, respectively (Figure 21). Immunolabeling showed that the binding of rRodA was more important on $\Delta rodA$ and ΔAR than on ΔPR or ΔAPR , suggesting that the presence of melanin favors the binding of RodA to the conidium (Figure 21b). Interestingly, monomeric soluble rRodA spontaneously self-assembled into a rodlet layer on the conidial surface as the one observed for *ku80* (Figure 21c). The coverage of the conidial layer with the rodlets was uncomplete (Figure 21c). Rodlets were seen on 20% of the conidia of the $\Delta rodA$ mutant and only on 8% of the conidia of ΔAPR mutant characterized by the absence of melanin. Binding of YWA1 was intense on $\Delta pksP$ and ΔAP , but was hardly detected if any on rodlet-minus ΔPR or ΔAPR mutants (Figure 21a). These results suggested that RodA and YWA1 need the presence of each other to be able to bind efficiently to *RODA* or *PKSP* deleted conidia, respectively, whereas neither, at least in our experimental conditions, rodlets and melanin interacted with α -(1,3)-glucan. These results also indicated that melanin and rodlets can associate on the conidial surface without the establishment of covalent linkages.

3 | DISCUSSION

The *A. fumigatus* conidia are the resistant airborne morphotype, which is responsible for the dissemination of the species and for the establishment of lung infection by this opportunistic fungal pathogen. The conidia are covered by RodA rodlets and melanin, allowing the buoyancy of the conidia in the air currents, masking the fungus from immune recognition, and protecting conidia against the host response (Aimanianda et al., 2009; Bayry et al., 2014). The rodlet and melanin layers coat a more inner component, which is the amorphous α -(1,3)-glucan. This glucan has a double opposite immune effect because it stimulates an anti-*A. fumigatus* immune response in murine models of aspergillosis or ex vivo using human T lymphocyte clones or dendritic cells (Bozza et al., 2009; Stephen-Victor, Bosschem, Haesebrouck, and Bayry, 2017a; Stephen-Victor, Karnam, et al., 2017b) but protects the fungus against phagocytosis (Beauvais et al., 2013). Germinated conidia lost melanin and rodlets layers, exposing the underneath layer composed of glycoproteins, chitin, and β -(1,3)-glucan. Exposition of these PAMPS on the conidial surface induced the activation of LAP, phagosome maturation, and fungal killing (Akoumianaki et al., 2016; Latgé, Beauvais, & Chamilos, 2017). In contrast, melanin blocks phagosome biogenesis and inhibits phagocyte apoptosis to provide an intracellular niche for conidial survival (Latgé et al., 2017). The removal of rodlets, melanin, or α -(1,3)-glucan made the conidia immunostimulatory but the immunological consequences of these mutations were different due to the specific immune effects of each of these components. For example, $\Delta rodA$, in spite of the partial exposure of β -(1,3)-glucans on the conidial surface which stimulate the anti-*A. fumigatus* host response, was still pathogenic in vivo in an invasive aspergillosis model in mice, because of the presence of α -(1,3)-glucan and melanin which are immunoprotective (Thau et al., 1994; Valsecchi, Dupres, et al., 2017). In contrast, $\Delta pksP$ or Δags had reduced virulence because of an increased susceptibility to defense effectors of the phagocytes, at least partly due to exposed

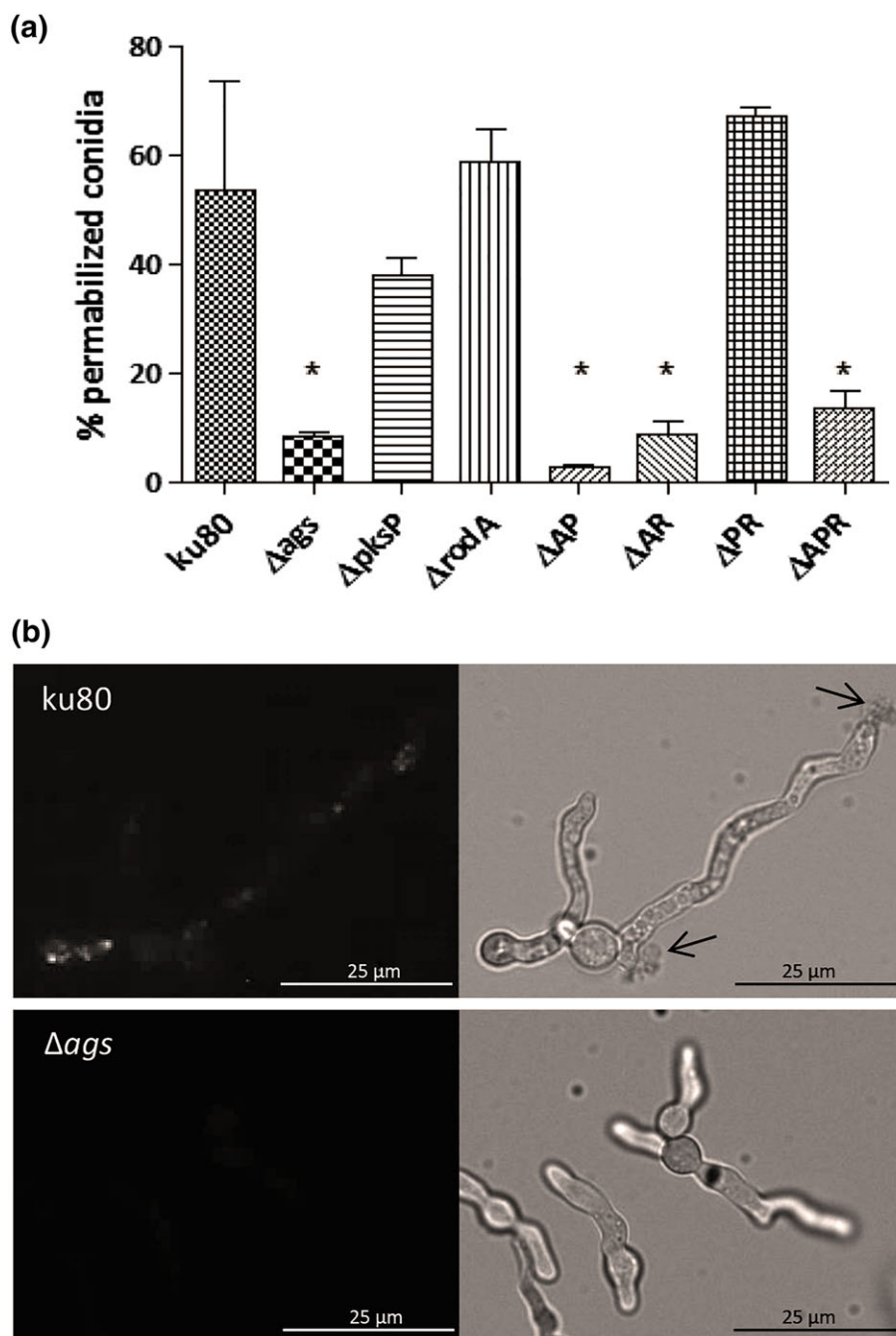


FIGURE 19 Permeability of *ku80* and mutants to CAS-DDAO, showing that the strains deleted in AGS genes were not permeable to this compound. (a) percent of positive cells to CAS-DDAO; * $p < 0.02$. (b) Fluorescence images of *ku80* and *Δags* germinated conidia incubated with CAS-DDAO for 3 hr at 37°C, showing lysis of hyphal-type compartments (arrows) and intracellular labelling only in *ku80*

glycoproteins (for *Δags* and *ΔpksP*) and chitin (for *ΔpksP*), which are two PAMPs that induce the early host defense reactions (Bayry et al., 2014; Beauvais et al., 2013; Jahn et al., 1997). Ex vivo, rodlet-deficient and melanin-deficient conidia of *A. fumigatus* triggered the production of high amounts of TNF and IL-1b in human monocytes (Akoumianaki et al., 2016).

The fact that melanin, RodA rodlets, and α -(1,3)-glucan are three major components of the outer layer involved in the resistance to the host antifungal response was the rationale for undertaking multiple deletions to construct a strain deficient in these three components, and consequently, in the outer layer of the conidium.

3.1 | Phenotypic modifications of the cell wall surface mutants

Multiple deletions of the genes coding for rodlets, melanin, and α -(1,3)-glucan lead to unexpected phenotypes.

First, in vitro survival of the fungus in air and water was not altered by the removal of melanin, α -(1,3)-glucans, and rodlets. It is interesting to note that this quintuple ΔAPR mutant is as resistant to desiccation in air as the parental strain, suggesting that compensatory mechanisms are in place in the mutant to keep water in the spore and substitute the putative function of this conidial outer layer. Strikingly,

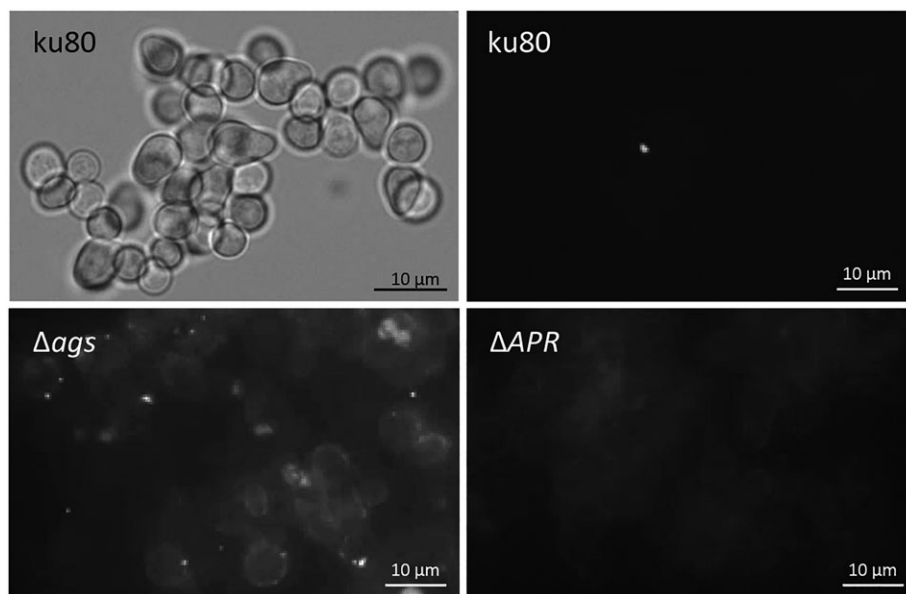


FIGURE 20 Permeabilization of *ku80*, Δ *ags* and Δ *APR* swollen conidia with POPC/DSPE-NBD liposomes, showing that only the strains deleted in AGS genes were permeable

our results indicate that conidial quiescence is independent of the physicochemical characteristics of the outer cell wall layer, which is hydrophobic and impermeable in the parental strain and sticky and hydrophilic in the quintuple Δ *APR* mutant. Hence, quiescence is directly under the control of intracellular molecular modules. Also unexpectedly, elimination of melanin (and rodlets), which constitutes a very tough shell resistant to all kinds of physicochemical insult and has to be degraded for the conidia to swell and germinate, does not speed up the germination process. These data suggested that the first step of germination, the conidial swelling, is induced by a high increase of the intracellular osmotic pressure which resulted in the disaggregation the rodlet-melanin layer. The higher rate of germination of the AGS deleted mutants (Δ *ags*, Δ *AP*, Δ *AR*, and Δ *APR*) suggested that in contrast to melanin and rodlets, α -(1,3)-glucan represented a barrier, opposite to the swelling effect resulting to the increase in the osmotic pressure, probably because of the elastic structure of this amorphous polysaccharide.

Second, the *in vitro* susceptibility of conidia to environmental stressors such as drugs, the *ex vivo* killing of conidia by monocytes are different. Specifically, when α -(1,3)-glucan and rodlets are depleted from the Δ *pksP* mutant, the susceptibility of the Δ *AP*, Δ *PR*, and Δ *APR* mutants to the phagocytic host response is similar to those of Δ *pksP*, demonstrating that the melanin is the major cell wall component protecting the fungus, and other mutations are not additive in terms of phagocytic resistance. Because *PKSP* deleted mutants adhered better to hydrophobic surfaces compared with the other strains (Figure 15), these also should be more adherent on phagocytic cells, favouring their phagocytosis rate, as described previously (Lamarre et al., 2009; Neves et al., 2017). Furthermore, our results provide evidence on a redundant mechanism of activation of the LAP pathway in response to difference cell wall immunostimulatory PAMPs and identify melanin as the dominant inhibitory molecule of the fungal cell wall targeting this pathway as previously observed (Akoumianaki et al., 2016). It has not been checked yet if chitin and

glycoproteins found on the surface of the Δ *pksP* mutant are capable of activating LAP. Following other immunostaining conditions on younger conidia (3 days old, YAG, 37°C), β -(1,3)-glucan has also been found on the surface of this Δ *pksP* mutant (Akoumianaki et al., 2016). The small increase seen in the killing of Δ *rodA*, Δ *ags*, and Δ *AR*, which did not result from LAP activation, could be due to the presence of immunostimulatory PAMPs such as chitin, β -(1,3)-glucan, and/or glycoproteins exposed on the surface of these mutants.

Third, structural compensatory reactions are seen when α -(1,3)-glucan and melanin, which are quantitatively the major components of the conidial outer layers, are both removed. These deletions induced an increase in the amount of the surface proteins in the Δ *AP* and Δ *APR* mutants, as well as a concomitant synthesis of GAG, which is a mycelial polysaccharide (Fontaine et al., 2011) that had never been found in the conidium.

Fourth, if one of the major conidial outer cell wall components is important for a particular phenotype, in most cases, genetic removal of the two other compounds does not significantly alter the phenotype. Nevertheless, some of the phenotypes observed for the conidia of the Δ *AP*, Δ *PR*, Δ *AR*, and Δ *APR* were unforeseen and did not seem to be induced by additive compensatory mechanisms. This is especially true for hydrophobicity, drug resistance, and cell wall permeability; three interdependent characteristics. The permeability of the cell wall to molecules is highly depending on the chemical nature of the drug and the compound used to analyze permeability. For example, melanin is the only compound that blocks the entrance of pyocyanin because only dormant Δ *pksP* conidia were permeable to pyocyanin, whereas Δ *rodA*, Δ *ags*, or *ku80* were not. Conversely, α -(1,3)-glucan controls the permeability to 50 nm liposomes because only Δ *ags*, Δ *AP*, Δ *AR*, and Δ *APR* were permeable to these. Similarly, Δ *ags* mutants were more sensitive to CR but more resistant to caspofungin. In contrast, Δ *rodA* and Δ *pksP* were more resistant to CR, but while Δ *pksP* was more resistant to caspofungin than the parental strain

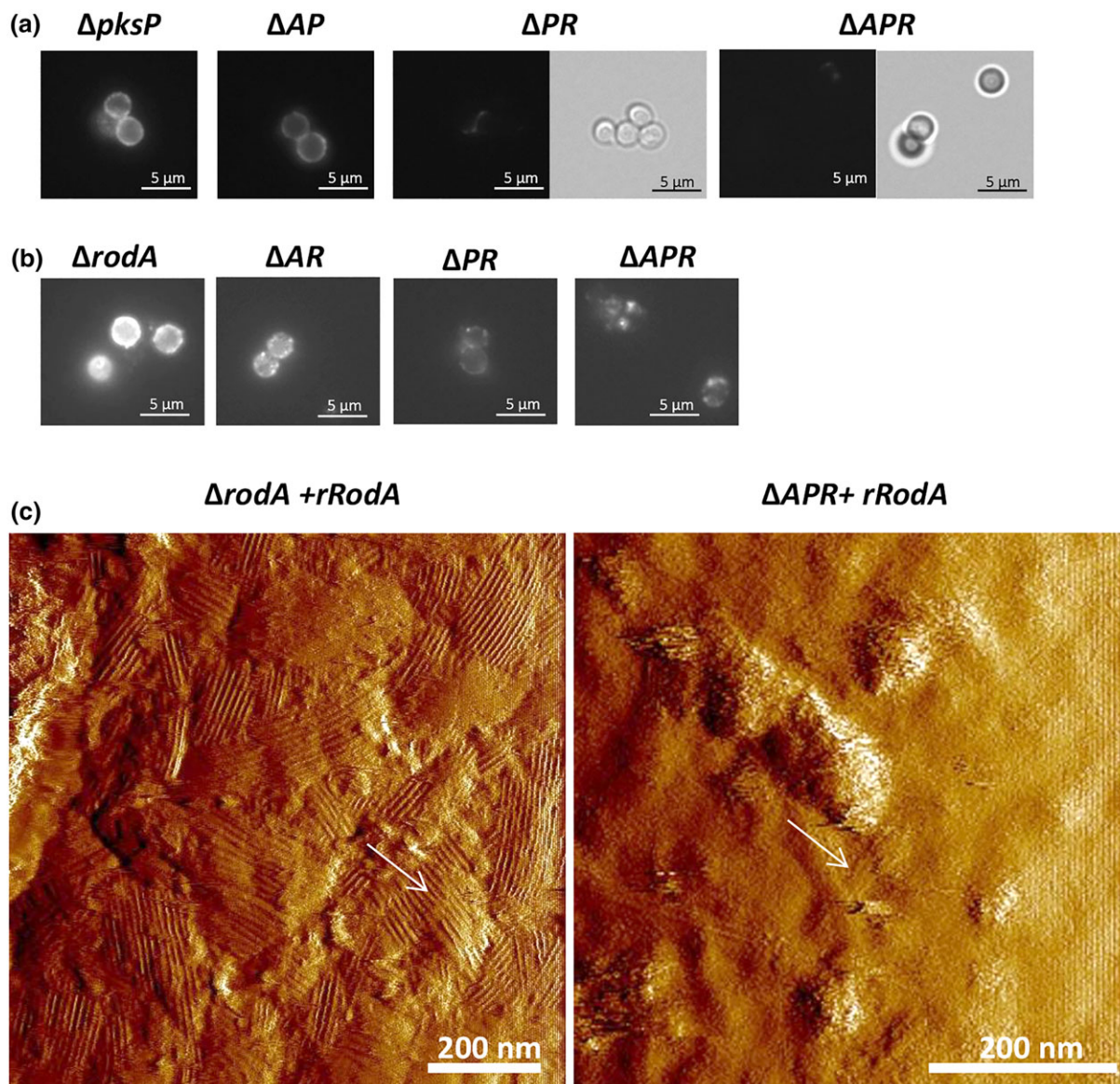


FIGURE 21 Interaction between melanin and RodA on the conidial cell wall surface. (a) Incubation of *PKSP* deleted conidia with the first melanin intermediate YWA1 and detection with MelLec-Fc and anti-human IgG-A488 Abs, showing the essentiality of the presence of RodA for YWA1 binding. (b,c) Incubation of *RODA* deleted conidia with the recombinant RodA protein (rRodA), anti-rRodA Abs, and anti-mouse IgG-Alexa 488 Abs (b) or imaged with AFM (c). Note the higher fluorescence on $\Delta rodA$ and ΔAPR (b) and the presence of more rodlets (arrows; c) in $\Delta rodA$ than in ΔAPR , showing the essentiality of the presence of melanin for RodA binding

ku80, $\Delta rodA$ showed the same sensitivity than ku80. Taking these observations into account, it is logical that ΔAP and ΔAR mutants are more sensitive to CR, but is difficult to rationalize that ΔAPR is more resistant.

The higher resistance to caspofungin of all the α -(1,3)-glucan knockout (Δags , ΔAP , ΔPR , ΔAR , and ΔAPR) mutants was also unexpected. Removal of α -(1,3)-glucan was associated with an increase in chitin in the Δags mutant (Henry et al., 2012) as well as in the ΔAP , ΔAR , and ΔAPR mutant cell wall (data not shown). Interestingly, *Candida albicans* cells with increased levels of cell wall chitin show reduced echinocandin susceptibility in vitro (Lee et al., 2012). It is tempting to think that resistance of the Δags mutants to caspofungin could also be due to an increase in chitin cell wall content.

3.2 | Structural organization of rodlets-melanin- α -(1,3)-glucan

The immunolabeling experiments with the anti α -(1,3)-glucan monoclonal IgA B-4.1 or the MelLec receptor showed a positive patchy labeling on ku80 dormant conidia covered with impermeable rodlets. This observation could be explained considering that both bulky probes were able to cross the rodlet layer to label the α -(1,3)-glucan or melanin present underneath the rodlet layer, or by the presence of some α -(1,3)-glucan and melanin epitopes emerging from the rodlet coat. In the $\Delta pksP$, $\Delta rodA$, and ΔPR mutants, conidia were negative to the B-4.1 mAb, indicating a structural reorganization of the cell wall upon gene deletion that hampers the access to the α -(1,3)-glucan epitope to this antibody. This could be linked to the

lack of modification of water efflux/influx in these mutants. Importantly, our data strongly suggest that RodA and melanin interact in the cell wall, and do so without any covalent linkage. RodA binding to the conidium was favored by the presence of melanin. Soluble monomeric RodA, added to rodlet-deficient cells ($\Delta rodA$, ΔAR), was able to spontaneously self-assemble into native rodlets at the surface of the spores, and the number of spores presenting rodlets was more important in spores with melanin. Similarly, the binding of YWA1 was more intense on cells with rodlets, suggesting that melanin assembly on the conidium surface could be favoured by the presence of rodlets. The biochemical characteristics of the interconnection between RodA and melanin are still unknown but the bonds between RodA and melanin are susceptible to formic acid, an acid able to dissociate noncovalently bound amyloid aggregates of RodA. In contrast to melanin and RodA, α -(1,3)-glucan oligomers did not bind to any mutant conidia. Recently, intermolecular interactions between α -(1,3)-glucan and chitin have been demonstrated in mycelia (Kang et al., 2018).

Compensatory mechanisms are seen when the cell wall composition is genetically modified due to the essential function of the cell wall for fungal life and the need to fight cell wall insults. A classical one is chitin synthesis, but other cell wall changes remain often unexplained (Latgé et al., 2017). Removal of α -(1,3)-glucan is associated with an increase in chitin (Henry et al., 2012). In spite of the importance of the melanin and rodlets in the conidial cell wall, $\Delta pksP$ and $\Delta rodA$ mutants do not show any modification of the cell wall polysaccharides (data not shown). The composition of the outer layer and the exposure of new different molecules on the conidial surface vary also with the genes deleted. The multiplicity of the gene deletion does not always, however, lead to a logical additivity of the phenotypes resulting from the successive deletions as shown in Table 1. The compensatory cell wall modifications can be totally unexpected as in the case of the ΔAP and ΔAPR mutants in which the lack of α -(1,3)-glucan and melanin is compensated by the presence of galactomannan on the conidial surface and the secretion of galactosaminogalactan, which is characteristically absent from the parental strain conidia. The three-dimensional structure of the outer cell wall requires now the use of more sophisticated physico-chemical instrumentation such as solid-state nuclear magnetic resonance or other approaches used for the analysis of the plant cell wall (Kang et al., 2018; Thomas et al., 2015).

4 | EXPERIMENTAL PROCEDURES

4.1 | Strains and culture conditions

The *A. fumigatus* reference strain used in this study is CEA17 ΔkuB^{ku80} ($ku80$)-deficient in nonhomologous end joining (da Silva Ferreira et al., 2006). This strain, which originates from the clinical isolate CBS 144-89, is as pathogenic as CBS 144-89 in experimental murine aspergillosis (da Silva Ferreira et al., 2006). The melanin ($\Delta pksP$)-deficient mutant, the rodlet ($\Delta rodA$)-deficient mutant, the triple α -(1,3)-glucan synthase mutant $\Delta ags1\Delta ags2\Delta ags3$ (Δags), and the $\Delta pksP\Delta rodA$ (ΔPR) mutant were previously obtained in our laboratory using $ku80$ as the parental strain (Akoumianaki et al., 2016; Henry et al., 2012; Kyrnizi et al., 2018; Valsecchi, Dupres, et al., 2017). The deletion mutants lacking either two or the three components (Table 4) were generated from the Δags (to obtain $\Delta ags\Delta pksP$ and $\Delta ags\Delta rodA$) or $\Delta ags\Delta rodA$ (to obtain $\Delta ags\Delta pksP\Delta rodA$) as described below. Strains were grown on 2% (w/v) malt agar slants. Dormant conidia were recovered in 0.05% (v/v) Tween 20 aqueous solution (Tw-H₂O) from the slants after three weeks at 25°C by vortexing, gently scraping the surface of the culture with an inoculation loop, and filtered using BD Falcon filters (BD Biosciences) to discard any mycelium resulting from the conidial recovery. Minimal medium (MM; Briard et al., 2015) was used for antifungal susceptibility, Sabouraud for germination (2% glucose, 1% Neopeptone; Difco), glucose 3%–yeast extract (1%) medium (GYE) for adherence test (Beauvais et al., 2007) and complete RPMI medium (10 mM Hepes, 1 mM sodium pyruvate, 25 mM glucose, 10% fetal calf serum, 2 mM L-glutamine, and 0.05 mM 2-mercaptoethanol) for primary human monocyte interaction study.

4.2 | Mutant constructions

The $\Delta ags\Delta pksP$ (ΔAP) and $\Delta ags\Delta rodA$ (ΔAR) deletion mutants were constructed on the Δags mutant background (Henry et al., 2012). To obtain ΔAP (s1), the ORF sequence of the *PKSP* gene in the Δags mutant was replaced by a 4,813 bp DNA construct. The construct and primers were both previously described (Akoumianaki et al., 2016). The construct contains the *PKSP* upstream (1,101 bp) and downstream borders (921 bp), as well as a chlorimuron ethyl marker

TABLE 4 Strains used in this study

Strain	Strain abbreviation	Deletion(s)
CEA17 ΔkuB^{ku80}	$ku80$	<i>KU80</i> (AFU2g02620)
$\Delta ags1\Delta ags2\Delta ags3$	Δags	<i>AGS1</i> (AFUA_3G00910), <i>AGS2</i> (AFUA_2G11270), <i>AGS3</i> (AFUA_1G15440)
$\Delta pksP$	$\Delta pksP$	<i>PKSP</i> (AFUA_2G17600)
$\Delta rodA$	$\Delta rodA$	<i>RODA</i> (AFUA_5G09580)
$\Delta ags\Delta pksP$	ΔAP	<i>AGS1</i> , <i>AGS2</i> , <i>AGS3</i> , <i>PKSP</i>
$\Delta ags\Delta rodA$	ΔAR	<i>AGS1</i> , <i>AGS2</i> , <i>AGS3</i> , <i>RODA</i>
$\Delta pksP\Delta rodA$	ΔPR	<i>PKSP</i> , <i>RODA</i>
$\Delta ags\Delta pksP\Delta rodA$	ΔAPR	<i>AGS1</i> , <i>AGS2</i> , <i>AGS3</i> , <i>PKSP</i> , <i>RODA</i>

[Chlori^R, 2,881 bp (Valent & Chumley, 1991)]. The Δ AR mutant (Figure S1B) was obtained by replacing the *RODA* gene in the Δ ags mutant by a DNA construct containing the PCRs of the *RODA* upstream and downstream borders and the chlorimuron-ethyl resistance β -recombinase [Chlori^R- β -rec, (Valsecchi, Sarikaya-Bayram, et al., 2017)]. The Geneart[®] Seamless Cloning and Assembly kit (Life Technologies) and the primers described in (Valsecchi, Dupres, et al., 2017) were used for assembling the construct.

To obtain the Δ ags Δ pksP Δ rodA (Δ APR) mutant, the Chlori^R- β -rec marker was first excised from Δ AR through the recombination of the *SIX* recognition regions by cultivating the mutant in MM containing 2% xylose. Proper excision of the selection marker was confirmed by PCR before transformation of Δ AR mutant with the 4813 bp *PKSP* borders-Chlori^R construct described above to replace of the *PKSP* ORF sequence (Figure S1C). All transformations were performed by electroporation as previously described (Lambou, Lamarre, Beau, Dufour, & Latge, 2010) and analyzed by diagnostic PRC and Southern blot using the DIG probe protocol (Roche diagnostics) as shown in Figure S1.

4.3 | Conidiation, survival, and germination analysis

Conidiation quantification and survival were done as previously described (Henry et al., 2016). Briefly, 3-week-old conidia at 25°C were recovered as described above from malt agar slants in Tw-H₂O (5 ml of Tw-H₂O were added to 10 ml slants) and quantified with a hemacytometer. To investigate the conidial survival, conidia were kept on malt agar slants or in Tw-H₂O for 3 months at 37°C, recovered and plated on Sabouraud agar medium. The percent of germination was determined after 9 hr incubation at 37°C. Conidial germination of the 3-week-old conidia at 25°C was evaluated on Sabouraud, MM, or GYE agar media at 37°C, and the percent of germination was determined over time until it reached 100%.

4.4 | Immunolabeling

Conidia were fixed with 2.5% *para*-formaldehyde (PFA) at 4°C overnight. After quenching of fixation with 0.1 M NH₄Cl, conidia were washed with phosphate-buffered saline (PBS), pH 7.0. Immunolabeling of fixed conidia was done in PBS-Tw containing 1% bovine serum albumin (PBS-Tw-BSA). The fixed conidia were first incubated for 30 min in PBS-Tw-BSA before adding the primary antibodies or receptors described below. After incubation for 1 hr, the conidia were washed and incubated in PBA-Tw-BSA with the secondary antibodies conjugated to a fluorochrome. After washing in PBS-Tw-BSA, the samples were observed under a wide-field epifluorescence microscope. For lectins labeling, fixed conidia were incubated with the lectins conjugated to a fluorochrome described below, in PBS-Tw for 15 min before washing in PBS-Tw and observation.

4.4.1 | RodA detection

For RodA detection, samples were immunolabeled with a primary polyclonal antiserum (Valsecchi, Dupres, et al., 2017; 1:250 dilution)

and a secondary anti-mouse IgG conjugated to Alexa488 (anti-mouse IgG-A488; Sigma).

4.4.2 | Melanin detection

MelLec is a melanin receptor used for melanin detection (Stappers et al., 2018). Conidia were incubated with a chimeric protein MelLec-Fc, which was kindly provided by G. Brown (University of Aberdeen, Aberdeen, United Kingdom). The receptor was immunolabeled with an anti-human Fc-IgG, coupled to Dylight 594 Ab (1:400 dilution).

4.4.3 | Chitin and glycoproteins detection

Chitin and glycoproteins were labeled with wheat germ agglutinin coupled with tetramethylrhodamine (WGA-TRITC) and concanavalin A labeled with fluorescein isothiocyanate (ConA-FITC), respectively, (Sigma) at 0.1 mg/ml.

4.4.4 | Galactofuranose-molecules detection

Galactofuranose, constitutive of galactomannan or galactomannoproteins, was labeled with a rat anti-galactofuranose (Galf) monoclonal antibody [EBA2, diluted 1:1,000, a kind gift of M. Tabouret from BioRad, Steenvorde (Stynen et al., 1992)] and revealed by anti-rat IgG-FITC (Jackson ImmunoResearch).

4.4.5 | β -(1,3)-glucan detection

To detect β -(1,3)-glucan, samples were incubated with dectin1-human IgG Fc chimeric β -(1,3)-glucan receptor (6 μ g/ml; kind gift of G. Brown, University of Aberdeen, United Kingdom) and immunolabeled with an anti-human Fc-IgG coupled to FITC (Fc-IgG-FITC; 1:200 dilution).

4.4.6 | α -(1,3)-Glucan detection

α -(1,3)-Glucan was detected by immunolabeling with the anti- α -(1,3)-glucan IgA monoclonal antibody B-4.1[kind gift of J. Kearney, University of Alabama, Birmingham, USA; (Kearney, McCarthy, Stohrer, Benjamin, & Briles, 1985)], or with the MOPC IgM [Sigma, 8 μ g/mL (Beauvais et al., 2013)], and revealed by the anti-mouse IgG-A488.

4.4.7 | Galactosaminogalactan detection

For galactosaminogalactan (GAG) detection, samples were immunolabeled with an anti-GAG mAb at 20 μ g/ml (Fontaine et al., 2011), which was detected with the anti-mouse IgG-A488 antibodies. Biochemical quantification of GAG was done on conidial cell wall extracts as previously described (Henry et al., 2012).

4.5 | Mass spectrometry analysis

For protein extraction, conidia were incubated in 60% formic acid for 10 min on ice. Dried samples were resuspended in 100 μ L of 8 M urea, 100 mM Tris-HCl pH 8.5. Samples were processed for mass spectrometry analysis and protein identification and quantification as

previously described (Jeannin et al., 2018). Raw results were analyzed with MaxQuant (Cox et al., 2011; Cox & Mann, 2008), and the protein group text output file was used for data analysis. For each replicate experiment, the values corresponding to contaminants or reverse protein sequences were removed. "Intensity" values were used for normalization and statistics computation. The signal was normalized to the sum of intensities in each experiment and the log₂-transformed values were used to calculate means for each protein, based on at least two independent experimental replicates. Transforms and data visualization were done with R. The mass spectrometry proteomics data have been deposited to the ProteomeXchange Consortium via the PRIDE partner repository with the dataset identifier PXD011734 (<https://cran.r-project.org/>).

4.6 | Analysis of the conidial surface by atomic force microscopy (AFM)

For atomic force microscopy (AFM) experiments, conidia were immobilized by mechanical trapping into isoporous polycarbonate membranes of 3 µm pores (Millipore), similar to conidial size. After filtering a spore suspension (20 ml; 10⁶ cells per ml), the membrane was carefully rinsed three times in deionized water and cut (1 cm × 1 cm). The lower part was carefully dried on a sheet of tissue and the specimen was attached to a steel sample puck using a small piece of adhesive tape. A droplet of liquid was rapidly added on the filter to avoid cell desiccation and the mounted sample was then transferred into the AFM liquid cell. Experiments were performed on a Multimode AFM (Bruker) in contact mode, in liquid, and at room temperature using a Nanoscope 8 equipment (Bruker, Santa Barbara, CA). Oxide-sharpened micro-fabricated silicon nitride (Si₃N₄) AFM probes with triangular cantilevers of stiffness 0.01 N/m were selected to image surfaces (MLCT-BIO-DC, Bruker, Santa Barbara, CA).

4.7 | Hydrophobicity measurement

Chemical force microscopy is a well-established approach that has been used to study the hydrophobicity of living microorganisms, including *A. fumigatus* (Dague et al., 2007; Noy, 2006). Hydrophobic tips were prepared as follows. Gold-coated cantilevers (OMCL-TR400PB, Olympus Ltd., Tokyo, Japan) were cleaned for 5 min using a Plasma-O₂ cleaner, rinsed with ethanol and dried with a gentle nitrogen flow. Gold-coated cantilevers were then immersed overnight in 1 mM solution of HS (CH₂)₁₁CH₃ in ethanol and then rinsed with ethanol. Conidia trapped in the membrane were then localized by contact mode using a silicon nitride tip. The bare tip was then changed with a hydrophobic tip to record adhesion force maps on the area of interest. At the end of the experiments, the spring constants of the cantilevers were measured using the thermal noise method (Nanoscope Analysis software, version 8.15, Bruker), yielding values ranging from 0.021 to 0.026 N/m. All force measurements were performed using a constant approach and retraction speed of 1,500 nm/s. Adhesion maps were obtained by recording 32 × 32 forces curves on 1 µm × 1 µm areas, calculating the adhesion force values and displaying them as grey pixels. Histograms were obtained by pooling the data from

several adhesion maps. Data analysis was done using in-house developed pyAF (python Atomic Force) software, version 1.5.1. All experiments were performed at least on four different conidia and with three different hydrophobic tips.

The percent of conidial hydrophobicity was also analyzed by adding 1 ml of H₂O to a 3-week-old malt tube culture at 25°C, the surface of the tube was vortexed for 30 s, gently scraped with an inoculation loop, and the water containing conidia was carefully recovered using a Pasteur pipet. One milliliter of Tw-H₂O was then added to the tube, which was vortexed for 30 s and Tw-H₂O containing conidia was recovered. The number of conidia was counted in each solution with a hemacytometer. The percentage of hydrophobic conidia was estimated with the formula: (number of conidia in H₂O/total number of Tw-H₂O conidia) × 100.

4.8 | Conidial adherence to polystyrene plates

Conidial adherence was tested on 48-well polystyrene plates as previously described (Valsecchi, Dupres et al., 2017): 300 µl conidia (10⁶/ml) were incubated in water for 1 hr in 48-well polystyrene plates (TPP, Thermofisher); the plates were then washed five times with water and the remaining adherent and non-adherent conidia were quantified by the resazurin method after 15 hr growth in GYE liquid medium at 37°C (Clavaud, Beauvais, Barbin, Munier-Lehmann, & Latgé, 2012).

4.9 | Susceptibility testing

Minimal effective concentration of caspofungin, a cell wall β-(1,3)-glucan synthesis inhibitor, and MIC of posaconazole and voriconazole, two ergosterol-synthesis inhibitors, were determined in MM agar according to the Clinical Laboratory Standards Institute M38-A2 protocol (NCCM) by the microdilution method in 96-well plates. Biomass growth was assessed using the redox indicator resazurin as previously described (Clavaud et al., 2012).

To test susceptibility to CR and CFW, 500 conidia were spotted on six-well microplates (Tissue culture plates, Sigma Aldrich) containing serial dilutions of CR or CFW in MM agar medium and incubated at 37°C in a humid chamber (Henry et al., 2016).

4.10 | Ex vivo experiments

4.10.1 | Isolation and stimulation of primary human monocytes

Healthy volunteers without any known infectious or inflammatory disorders donated blood. Monocytes from healthy controls were isolated from PBMCs using magnetic bead separation with anti-CD14 coated beads (MACS Miltenyi Germany) according to the protocol supplemented by the manufacturer. The monocytes were resuspended in RPMI culture medium, supplemented with 1% gentamicin, 1% L-glutamine, and 1% pyruvate. The cells were counted in a Bürker counting chamber, and their number was adjusted to 2 × 10⁶/ml. A total of 1 × 10⁵ treated monocytes per condition in a final volume of 200 µl were allowed to adhere to polylysine glass coverslips (Ø 12 mm) for

1 hr followed by stimulation with *A. fumigatus* conidia of the indicated strain at a multiplicity of infection (MOI) of 3:1 at 37°C for the indicated time point. After stimulation, cells were washed twice with PBS to remove medium and nonphagocytosed spores and cells were fixed on the coverslips for 15 min in 4% paraformaldehyde. Subsequently the coverslips were washed with PBS followed by a fixation in ice cold methanol for 10 min at -20°C, after which, cover slips were be stored in PBS at 4°C until immunofluorescence staining.

4.10.2 | Immunofluorescence experiments

Conidia were labeled with FITC as previously described (Akoumianaki et al., 2016). Briefly, freshly harvested conidia ($5 \times 10^7/2$ ml of 50 mM Na carbonate buffer, pH 10.2) were incubated with FITC (0.1 mg/ml final concentration) at 37°C for 1 hr and washed by centrifugation three times in PBS-0.1% Tween 20. When needed, inactivation of fungal conidia was done by exposure to 4% PFA (2 hr, room temperature) followed by treatment with 100 mM glycine in PBS and three washes in PBS and verified by CFU plating. We have previously validated that PFA-inactivation of *A. fumigatus* conidia does not affect surface exposure of β -glucan, dectin-1 signaling activation, cytokine responses, and melanin inhibitory action on LAP (Akoumianaki et al., 2016).

For immunofluorescence imaging, cells were seeded on coverslips pretreated with polylysine, fixed with 4% PFA for 15 min in room temperature followed by 10 min of fixation with ice cold methanol at -20°C, washed twice with PBS, permeabilized with 0.1% saponin (Sigma). After blocking the permeabilization with a 30 min incubation in PBS-BSA (PBS + 2% BSA), samples were incubated for 1 hr with the primary antibody: a-LC3B (clone 5F10, Nanotools; dilution 1:20) or the inhibitor a-p47phox (610354 BD; dilution 1:100), washed twice in PBS-BSA, stained by the appropriate secondary AlexaFluor secondary Ab (Molecular Probes), followed by DNA staining with 10 μ M TOPRO-3 iodide (642/661; Invitrogen). After the washing steps, slides were mounted in Prolong Gold antifade media (Molecular Probes). Images were acquired using a laser-scanning spectral confocal microscope (TCS SP2; Leica), LCS Lite software (Leica), and a 40 \times Apochromat 1.25 NA oil objective using identical gain settings. A low-fluorescence immersion oil (11513859; Leica) was used, and imaging was performed at room temperature. Serial confocal sections at 0.5 μ m steps within a z-stack, spanning a total thickness of 10 to 12 μ m of the cell, were taken to assess for internalized conidia contained within phagosomes. Unless otherwise stated, mean projections of image stacks were obtained using the LCS Lite software and processed with Adobe Photoshop CS2. Phagosomes surrounded by a rim of fluorescence of the indicated protein-marker were scored as positive, according to established protocols in our lab. At least 200 phagosomes were analyzed for each experimental condition in three independent experiments.

4.10.3 | Measurement of reactive oxidants production

Reactive oxidant measurements were performed by means of a dichlorofluorescein assay (Akoumianaki et al., 2016). Stock solution of dichlorofluorescein diacetate (DCFH-DA) was dissolved in dimethyl

sulfoxide (DMSO) to a final concentration of 100 mM. Human monocytes (2×10^5 /well) were plated on 96-well round bottom plates, incubated at 37°C for 30 min and stimulated for 1 hr with *A. fumigatus* PFA-fixed conidia (in order to prevent changes in cell wall surface composition) of the indicated strain in the presence of DCFH-DA added to a final concentration of 10 μ M during the last 30 min. After 30 min of exposure, the content of the wells was transferred to vials and the fluorescence of the cells from each well measured by flow cytometry. Cells were acquired on a FACSCalibur (BD Biosciences) and analyzed using the FlowJo software (Tree Star).

4.10.4 | Killing of *A. fumigatus* by primary human monocytes

Primary human monocytes (2×10^5 /well) were plated onto 96-well round bottom plates for 1 hr, and subsequently infected with the live conidia at an MOI of 1:10 (conidia: monocyte ratio) for 1 hr at 37°C. Medium containing non-adherent, nonphagocytosed conidia was removed, wells were washed three times using warm PBS, and new medium was added. Monocytes were then allowed to kill conidia for 24 hr before intracellular conidia were harvested by lysis of monocytes with 0.5% Triton-X. The process of cellular lysis was confirmed by light microscopy and killing of *A. fumigatus* conidia was assessed by CFU plating. The experiment was performed in quadruplicate with monocytes obtained from four different donors.

Approval for the collection of blood for functional studies on monocytes was obtained from the Ethics Committee of the University Hospital of Heraklion, Crete, Greece (5159/2014). All individuals provided written informed consent in accordance with the Declaration of Helsinki.

4.11 | POPC/DSPE-NBD Liposome preparation

Liposome formulations made of 1-palmitoyl-2-oleoyl-sn-glycero-3-phosphocholine-1-oleoyl-2-[12-[(7-nitro-2-1,3-benzoxadiazol-4-yl)amino] dodecanoyl]-sn-glycero-3-phosphoethanolamine (POPC/DSPE-NBD) at 99/1 molar proportions were prepared according to the Bangham's method followed by extrusion of vesicle suspensions (Bangham, Standish, & Watkins, 1965). Briefly, lipids (10 mM) were dispersed in chloroform. Organic lipid solutions were evaporated for 3 hr at 60°C under reduced pressure. The resulting dry lipid films were hydrated with PBS buffer and sonicated for a few minutes. The obtained POPC/DSPE-NBD liposome suspensions were then extruded 15 times successively through 400 and 200 nm pore-diameter polycarbonate membranes at 40°C (Mini extruder, Avanti Polar Lipids, Alabaster, AL). The diameter of liposomes was 50 nm as measured by diffusion light scattering using a Zeta-sizer (Nano ZS90, Malvern) after dilution of the suspension in buffer.

4.12 | Permeability assays with pyocyanin, liposomes, and caspofungin

Penetration of pyocyanin and liposomes into swollen conidia was done as previously described (Briard et al., 2015). Briefly, swollen

conidia obtained after incubating conidia in GYE medium for 2 hr at 37°C were incubated further for 2 hr at 37°C with 2 mM pyocyanin (Sigma) or 0.5 mM POPC/DSPE-NBD liposomes. After washing with PBS, the samples were observed under UV light for pyocyanin or with an FITC filter for NBD fluorescence.

To test the permeability of the strains to caspofungin, we used 1,3-dichloro-9,9-dimethyl acridin-2-one conjugated to caspofungin [CAS-DDAO; a kind gift from D. Perlin, Public Health Research Institute, Newark, New Jersey, USA (Pratt et al., 2013)]. Germinated conidia were prepared in eight-well glass bottom treated Ibidi μ -slides by inoculating 2×10^5 conidia/ml for 10 hr in 250 μ l of MM medium and then incubated with 2 μ l of CAS-DDAO 1 mM directly added in the 250 μ l of culture. After 3 hr at 37°C, the fluorescent germinated conidia were counted using a green fluorescent protein light setting.

4.13 | Binding of oligo- α -(1,3)-glucan, the melanin intermediate YWA1, and recombinant RodA to mutant conidia

Because α -(1,3)-glucan are insoluble in non-alkali-solutions, oligomers of α -(1,3)-glucan (7, 9, and 11 hexoses units) conjugated to biotin were used (kind gift of N. Nifantiev, Russian Academy of Sciences, Leninsky prospect 47, 119991 Moscow, Russia). Five micrograms were incubated with 10^6 conidia for 2 hr at room temperature in PBS-Tw. After PBS-Tw washing, binding of the α -(1,3)-glucan oligomers was detected with Cy3-conjugated streptavidin (Jackson Immuno Research) and observed under a wide-field fluorescent microscope.

Heptaketide naphthopyrone (YWA1), the precursor of DHN-melanin, was purified as described previously (Tsai et al., 2001). Two micrograms of YWA1 were incubated with 10^6 conidia for 2 hr at room temperature in PBS-Tw, and the binding was detected using the MelLec receptor as described above (4.4.2).

Recombinant RodA (rRodA; 10 μ g) prepared as previously described (Valsecchi, Dupres, et al., 2017), was incubated with 10^6 conidia 2 hr at room temperature in PBS-Tw. Binding was detected using the polyclonal antibodies as described above (4.4.1).

4.14 | Statistical analysis

The data were expressed as means \pm SEM. Statistical significance of differences was determined by two-tailed Student's *t*-test and one-way ANOVA, with the indicated post-hoc test for multiple comparisons ($p < 0.05$ were considered statistically significant). Analysis was done with GraphPad Prism.

ACKNOWLEDGEMENT

Researches in the Aspergillus Unit, the Biological NMR Platform (formerly in the Unité de RMN des Biomolécules) and the Centre for Infection and Immunity were supported by the Institut Pasteur Research Transversal Program PTR 529. Works in the Biological NMR platform and the Centre for Infection and Immunity were

additionally funded by the French ANR FUNHYDRO ANR-16S-CE110020-01 and ANR 10-EQPX-04-01 respectively.

CONFLICT OF INTEREST

None.

ORCID

Cosmin Saveanu  <https://orcid.org/0000-0002-1677-7936>

Anne Beauvais  <https://orcid.org/0000-0002-2913-2213>

REFERENCES

- Aimanianda, V., Bayry, J., Bozza, S., Kniemeyer, O., Perruccio, K., Elluru, S. R., ... Latgé, J. P. (2009). Surface hydrophobin prevents immune recognition of airborne fungal spores. *Nature*, 460, 1117–1121. <https://doi.org/10.1038/nature08264>
- Akoumianaki, T., Kyrnizi, I., Valsecchi, I., Gresnigt, M. S., Samonis, G., Drakos, E., ... Chamilos, G. (2016). *Aspergillus* cell wall melanin blocks lc3-associated phagocytosis to promote pathogenicity. *Cell Host & Microbe*, 19, 79–90. <https://doi.org/10.1016/j.chom.2015.12.002>
- Bangham, A. D., Standish, M. M., & Watkins, J. C. (1965). Diffusion of univalent ions across the lamellae of swollen phospholipids. *Journal of Molecular Biology*, 13, 238–252.
- Bayry, J., Beaussart, A., Dufrêne, Y. F., Sharma, M., Bansal, K., Kniemeyer, O., ... Beauvais, A. (2014). Surface structure characterization of *Aspergillus fumigatus* conidia mutated in the melanin synthesis pathway and their human cellular immune response. *Infection and Immunity*, 82, 3141–3153. <https://doi.org/10.1128/IAI.01726-14>
- Beaussart, A., El-Kirat-Chatel, S., Fontaine, T., Latgé, J.-P., & Dufrêne, Y. F. (2015). Nanoscale biophysical properties of the cell surface galactosaminogalactan from the fungal pathogen *Aspergillus fumigatus*. *Nanoscale*, 7, 14996–15004.
- Beauvais, A., Bozza, S., Kniemeyer, O., Formosa, C., Formosa, C., Balloy, V., et al. (2013). Deletion of the α -(1,3)-glucan synthase genes induces a restructuring of the conidial cell wall responsible for the avirulence of *Aspergillus fumigatus*. *PLoS Pathogens*, 9, e1003716. <https://doi.org/10.1371/journal.ppat.1003716>
- Beauvais, A., Schmidt, C., Guadagnini, S., Roux, P., Perret, E., Henry, C., ... Latgé, J. P. (2007). An extracellular matrix glues together the aerial-grown hyphae of *Aspergillus fumigatus*. *Cellular Microbiology*, 9, 1588–1600. <https://doi.org/10.1111/j.1462-5822.2007.00895.x>
- Bozza, S., Clavaud, C., Giovannini, G., Fontaine, T., Beauvais, A., Sarfati, J., et al. (2009). Immune sensing of *Aspergillus fumigatus* proteins, glycolipids, and polysaccharides and the impact on Th immunity and vaccination. *J Immunol Baltim Md*, 1950(183), 2407–2414.
- Briard, B., Bomme, P., Lechner, B. E., Mislin, G. L. A., Lair, V., Prévost, M.-C., ... Beauvais, A. (2015). *Pseudomonas aeruginosa* manipulates redox and iron homeostasis of its microbiota partner *Aspergillus fumigatus* via phenazines. *Scientific Reports*, 5, 8220.
- Bubis, J. A., Levitsky, L. I., Ivanov, M. V., Tarasova, I. A., & Gorshkov, M. V. (2017). Comparative evaluation of label-free quantification methods for shotgun proteomics. *Rapid Commun Mass Spectrom RCM*, 31, 606–612. <https://doi.org/10.1002/rcm.7829>
- Clavaud, C., Beauvais, A., Barbin, L., Munier-Lehmann, H., & Latgé, J.-P. (2012). The composition of the culture medium influences the β -1,3-glucan metabolism of *Aspergillus fumigatus* and the antifungal activity of inhibitors of β -1,3-glucan synthesis. *Antimicrobial Agents and Chemotherapy*, 56, 3428–3431.
- Cox, J., & Mann, M. (2008). MaxQuant enables high peptide identification rates, individualized p.p.b.-range mass accuracies and proteome-wide protein quantification. *Nature Biotechnology*, 26, 1367–1372.
- Cox, J., Neuhauser, N., Michalski, A., Scheltema, R. A., Olsen, J. V., & Mann, M. (2011). Andromeda: A peptide search engine integrated into the MaxQuant environment. *Journal of Proteome Research*, 10, 1794–1805.

- da Silva Ferreira, M. E., Kress, M. R. V. Z., Savoldi, M., Goldman, M. H. S., Härtl, A., Heinekamp, T., ... Goldman, G. H. (2006). The akuB (KU80) mutant deficient for nonhomologous end joining is a powerful tool for analyzing pathogenicity in *Aspergillus fumigatus*. *Eukaryotic Cell*, 5, 207–211. <https://doi.org/10.1128/EC.5.1.207-211.2006>
- Dague, E., Alsteens, D., Latgé, J.-P., & Dufrêne, Y. F. (2008). High-resolution cell surface dynamics of germinating *Aspergillus fumigatus* conidia. *Biophysical Journal*, 94, 656–660.
- Dague, E., Alsteens, D., Latgé, J.-P., Verbelen, C., Raze, D., Baulard, A. R., & Dufrêne, Y. F. (2007). Chemical force microscopy of single live cells. *Nano Letters*, 7, 3026–3030.
- Fontaine, T., Delangle, A., Simenel, C., Coddeville, B., van Vliet, S. J., van Kooyk, Y., ... Latgé, J. P. (2011). Galactosaminogalactan, a new immunosuppressive polysaccharide of *Aspergillus fumigatus*. *PLoS Pathogens*, 7, e1002372
- Gravelat, F. N., Beauvais, A., Liu, H., Lee, M. J., Snarr, B. D., Chen, D., ... Sheppard, D. C. (2013). *Aspergillus* galactosaminogalactan mediates adherence to host constituents and conceals hyphal β -glucan from the immune system. *PLoS Pathogens*, 9, e1003575. <https://doi.org/10.1371/journal.ppat.1003575>
- Henry, C., Fontaine, T., Heddergott, C., Robinet, P., Aïmanianda, V., Beau, R., ... Latgé, J. P. (2016). Biosynthesis of cell wall mannan in the conidium and the mycelium of *Aspergillus fumigatus*. *Cellular Microbiology*, 18, 1881–1891. <https://doi.org/10.1111/cmi.12665>
- Henry, C., Latgé, J.-P., & Beauvais, A. (2012). α 1,3 glucans are dispensable in *Aspergillus fumigatus*. *Eukaryotic Cell*, 11, 26–29.
- Jahn, B., Koch, A., Schmidt, A., Wanner, G., Gehring, H., Bhakdi, S., & Brakhage, A. A. (1997). Isolation and characterization of a pigmentless-conidium mutant of *Aspergillus fumigatus* with altered conidial surface and reduced virulence. *Infection and Immunity*, 65, 5110–5117.
- Jeannin, P., Chaze, T., Gai Gianetto, Q., Matondo, M., Gout, O., Gessain, A., & Afonso, P. V. (2018). Proteomic analysis of plasma extracellular vesicles reveals mitochondrial stress upon HTLV-1 infection. *Scientific Reports*, 8, 5170.
- Johnson, M. E., & Edlind, T. D. (2012). Topological and mutational analysis of *Saccharomyces cerevisiae* Fks1. *Eukaryotic Cell*, 11, 952–960.
- Kang, X., Kirui, A., Muszyński, A., Widanage, M. C. D., Chen, A., Azadi, P., ... Wang, T. (2018). Molecular architecture of fungal cell walls revealed by solid-state NMR. *Nature Communications*, 9, 2747. <https://doi.org/10.1038/s41467-018-05199-0>
- Kearney, J. F., McCarthy, M. T., Stohrer, R., Benjamin, W. H., & Briles, D. E. (1985). Induction of germ-line anti-alpha 1-3 dextran antibody responses in mice by members of the Enterobacteriaceae family. *J Immunol Baltim Md* 1950, 135, 3468–3472.
- Kyrmizi, I., Ferreira, H., Carvalho, A., Figueroa, J. A. L., Zampas, P., Cunha, C., ... Chamilos, G. (2018). Calcium sequestration by fungal melanin inhibits calcium-calmodulin signalling to prevent LC3-associated phagocytosis. In *Nat Microbiol* (ed., Vol. 3) (pp. 791–803). <https://doi.org/10.1038/s41564-018-0167-x>
- Lamarre, C., Beau, R., Balloy, V., Fontaine, T., Wong Sak Hoi, J., Guadagnini, S., ... Latgé, J. P. (2009). Galactofuranose attenuates cellular adhesion of *Aspergillus fumigatus*. *Cellular Microbiology*, 11, 1612–1623. <https://doi.org/10.1111/j.1462-5822.2009.01352.x>
- Lamarre, C., Sokol, S., Debeaupuis, J.-P., Henry, C., Lacroix, C., Glaser, P., ... Latgé, J. P. (2008). Transcriptomic analysis of the exit from dormancy of *Aspergillus fumigatus* conidia. *BMC Genomics*, 9, 417. <https://doi.org/10.1186/1471-2164-9-417>
- Lambou, K., Lamarre, C., Beau, R., Dufour, N., & Latgé, J.-P. (2010). Functional analysis of the superoxide dismutase family in *Aspergillus fumigatus*. *Molecular Microbiology*, 75, 910–923.
- Latgé, J.-P., & Beauvais, A. (2014). Functional duality of the cell wall. *Current Opinion in Microbiology*, 20, 111–117.
- Latgé, J.-P., Beauvais, A., & Chamilos, G. (2017). The cell wall of the human fungal pathogen *Aspergillus fumigatus*: Biosynthesis, organization, immune response, and virulence. *Annu Rev Microbiol*, 71, 99–116.
- Lee, K. K., Maccallum, D. M., Jacobsen, M. D., Walker, L. A., Odds, F. C., Gow, N. A. R., & Munro, C. A. (2012). Elevated cell wall chitin in *Candida albicans* confers echinocandin resistance in vivo. *Antimicrobial Agents and Chemotherapy*, 56, 208–217.
- Millet, N., Latgé, J.-P., & Mouyna, I. (2018). Members of glycosyl-hydrolase family 17 of *A. fumigatus* differentially affect morphogenesis. *J Fungi Basel Switz*, 4. <https://doi.org/10.3390/jof4010018>
- Moreno-Velásquez, S. D., Seidel, C., Juvvadi, P. R., Steinbach, W. J., & Read, N. D. (2017). Caspofungin-mediated growth inhibition and paradoxical growth in *Aspergillus fumigatus* involve fungicidal hyphal tip lysis coupled with regenerative intrahyphal growth and dynamic changes in β -1,3-glucan synthase localization. *Antimicrobial Agents and Chemotherapy*, 61.
- Neves, G. W. P., Curty, N. d. A., Kubitschek-Barreira, P. H., Fontaine, T., Souza, G. H. M. F., Cunha, M. L., ... Lopes-Bezerra, L. M. (2017). Modifications to the composition of the hyphal outer layer of *Aspergillus fumigatus* modulates HUVEC proteins related to inflammatory and stress responses. *Journal of Proteomics*, 151, 83–96. <https://doi.org/10.1016/j.jprot.2016.06.015>
- Noy, A. (2006). Chemical force microscopy of chemical and biological interactions. *Surface and Interface Analysis*, 1429–1441.
- Paris, S., Debeaupuis, J.-P., Crameri, R., Carey, M., Charlès, F., Prévost, M. C., ... Latgé, J. P. (2003). Conidial hydrophobins of *Aspergillus fumigatus*. *Applied and Environmental Microbiology*, 69, 1581–1588. <https://doi.org/10.1128/AEM.69.3.1581-1588.2003>
- Pratt, A., Garcia-Effron, G., Zhao, Y., Park, S., Mustae, A., Pillai, S., & Perlin, D. S. (2013). Evaluation of fungal-specific fluorescent labeled echinocandin probes as diagnostic adjuncts. *Medical Mycology*, 51, 103–107.
- Singh, B., Oellerich, M., Kumar, R., Kumar, M., Bhadoria, D. P., Reichard, U., ... Asif, A. R. (2010). Immuno-reactive molecules identified from the secreted proteome of *Aspergillus fumigatus*. *Journal of Proteome Research*, 9, 5517–5529. <https://doi.org/10.1021/pr100604x>
- Stappers, M. H. T., Clark, A. E., Aïmanianda, V., Bidula, S., Reid, D. M., Asamaphan, P., ... Brown, G. D. (2018). Recognition of DHN-melanin by a C-type lectin receptor is required for immunity to *Aspergillus*. *Nature*, 555, 382–386. <https://doi.org/10.1038/nature25974>
- Stephen-Victor, E., Bosschem, I., Haesebrouck, F., & Bayry, J. (2017). The Yin and Yang of regulatory T cells in infectious diseases and avenues to target them. *Cellular Microbiology*, 19.
- Stephen-Victor, E., Karnam, A., Fontaine, T., Beauvais, A., Das, M., Hegde, P., ... Bayry, J. (2017). *Aspergillus fumigatus* cell wall α -(1,3)-glucan stimulates regulatory T-cell polarization by inducing PD-L1 expression on human dendritic cells. *The Journal of Infectious Diseases*, 216, 1281–1294. <https://doi.org/10.1093/infdis/jix469>
- Stylen, D., Sarfati, J., Goris, A., Prévost, M. C., Lesourd, M., Kamphuis, H., ... Latgé, J. P. (1992). Rat monoclonal antibodies against *Aspergillus* galactomannan. *Infection and Immunity*, 60, 2237–2245.
- Suh, M.-J., Fedorova, N. D., Cagas, S. E., Hastings, S., Fleischmann, R. D., Peterson, S. N., ... Momany, M. (2012). Development stage-specific proteomic profiling uncovers small, lineage specific proteins most abundant in the *Aspergillus fumigatus* conidial proteome. *Proteome Science*, 10, 30. <https://doi.org/10.1186/1477-5956-10-30>
- Thau, N., Monod, M., Crestani, B., Rolland, C., Tronchin, G., Latgé, J. P., & Paris, S. (1994). Rodletless mutants of *Aspergillus fumigatus*. *Infection and Immunity*, 62, 4380–4388.
- Thomas, L. H., Forsyth, V. T., Martel, A., Grillo, I., Altaner, C. M., & Jarvis, M. C. (2015). Diffraction evidence for the structure of cellulose microfibrils in bamboo, a model for grass and cereal celluloses. *BMC Plant Biology*, 15, 153.
- Tsai, H. F., Fujii, I., Watanabe, A., Wheeler, M. H., Chang, Y. C., Yasuoka, Y., ... Kwon-Chung, K. J. (2001). Pentaketide melanin biosynthesis in *Aspergillus fumigatus* requires chain-length shortening of a heptaketide precursor. *The Journal of Biological Chemistry*, 276, 29292–29298. <https://doi.org/10.1074/jbc.M101998200>

- Valent, B., & Chumley, F. G. (1991). Molecular genetic analysis of the rice blast fungus, *magnaporthe grisea*. *Annu Rev Phytopathol*, 29, 443–467.
- Valsecchi, I., Dupres, V., Stephen-Victor, E., Guijarro, J. I., Gibbons, J., Beau, R., ... Beauvais, A. (2017). Role of hydrophobins in *Aspergillus fumigatus*. *J Fungi*, 4, 2. <https://doi.org/10.3390/jof4010002>
- Valsecchi, I., Sarikaya-Bayram, Ö., Wong Sak Hoi, J., Muszkiet, L., Gibbons, J., Prevost, M.-C., ... Latgé, J. P. (2017). MybA, a transcription factor involved in conidiation and conidial viability of the human pathogen *Aspergillus fumigatus*. *Molecular Microbiology*, 105, 880–900. <https://doi.org/10.1111/mmi.13744>

SUPPORTING INFORMATION

Additional supporting information may be found online in the Supporting Information section at the end of the article.

How to cite this article: Valsecchi I, Dupres V, Michel J-P, et al. The puzzling construction of the conidial outer layer of *Aspergillus fumigatus*. *Cellular Microbiology*. 2019;21:e12994. <https://doi.org/10.1111/cmi.12994>